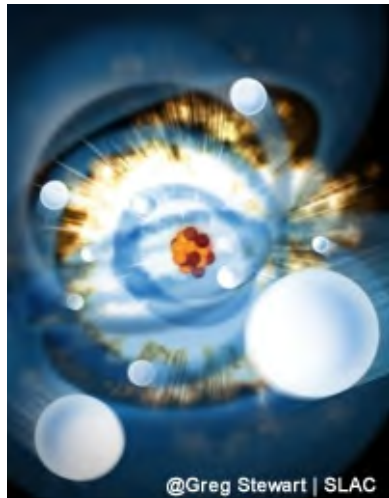


Atomic and molecular physics using ultrafast x-rays

Linda Young



Ultrafast X-ray Summer School
DESY Hamburg
23 Jun 2011

Outline

- Why are we here? What is so exciting about ultrafast x-rays in atomic and molecular physics?
- Review some basic x-ray processes in atoms
- Extension to the strong-field regime for x-rays
 - Optical-control of x-ray processes
 - X-ray induced processes
- Quiz



Some General References:

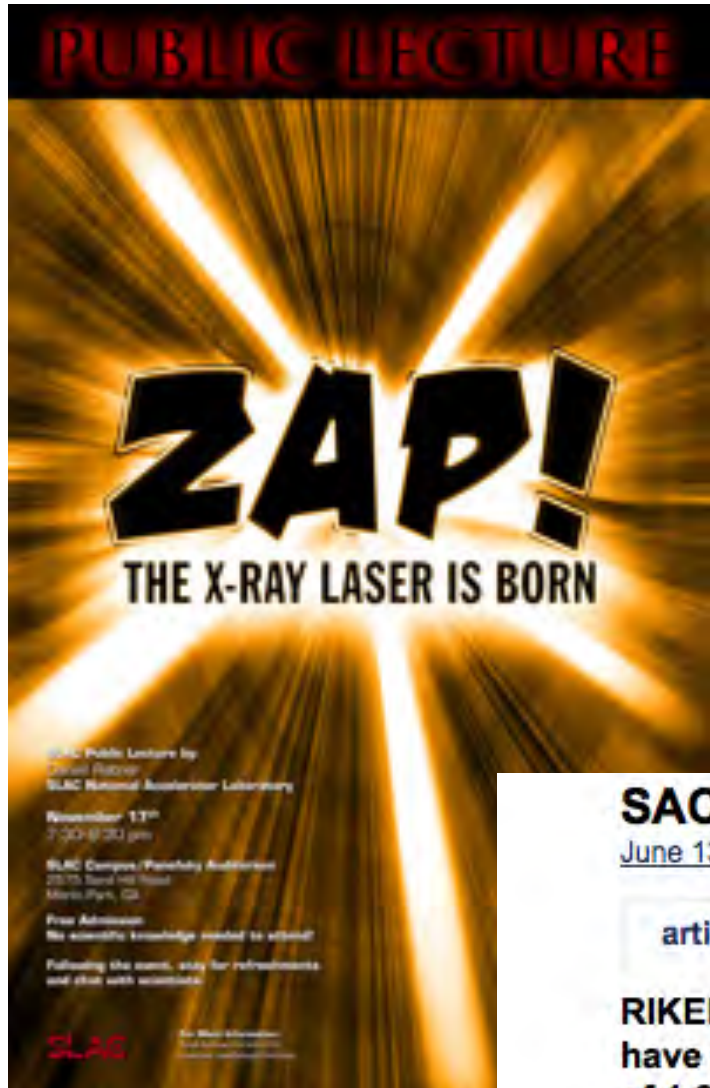
Ultrafast “optical” lasers and strong field studies

- “Intense few cycle laser fields: frontiers of nonlinear optics”
T. Brabec & F. Krausz, Rev Mod Phys **72**, 545 (2000)
- “Attosecond physics”
F. Krausz & M. Ivanov, Rev Mod Phys **81**, 163 (2009)

Basic concepts of x-ray atom interactions

- “Concepts in x-ray Physics”
R. Santra J Phys B 42, 023001 (2009)
- Electron Spectrometry of Atoms using Synchrotron Radiation
V. Schmidt (Cambridge University Press, 1997)





SACLA X-ray free electron laser sets new record

[June 13, 2011](#)

[article](#)

[comments \(0\)](#)

[text-to-speech](#)

[share](#)

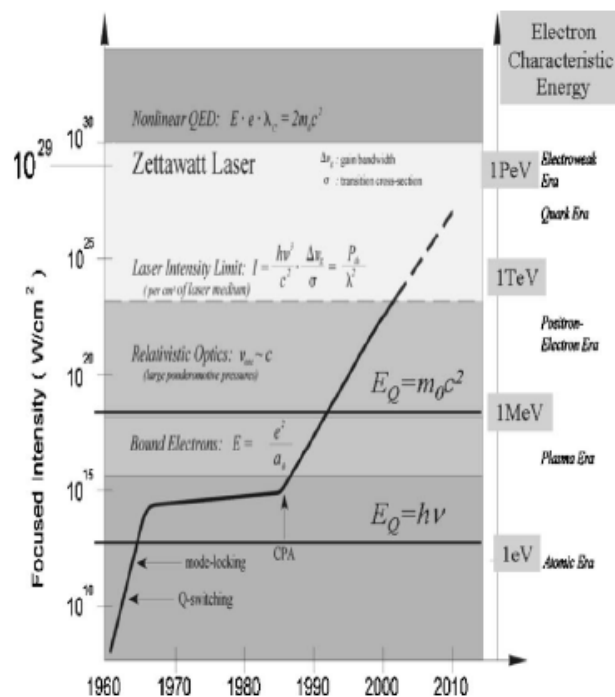
RIKEN and the Japan Synchrotron Radiation Research Institute (JASRI) have successfully produced a beam of X-ray laser light with a wavelength of 1.2 Angstroms, the shortest ever measured. This record-breaking light was created using SACLA, a cutting-edge X-ray Free Electron Laser (XFEL) facility unveiled by RIKEN in February 2011 in Harima, Japan. SACLA (SPring-8 Angstrom Compact free electron LAser) opens a window into the structure of atoms and molecules at a level of detail never seen before.



Compare the evolution of high intensity optical and x-ray sources

High-intensity at optical wavelengths

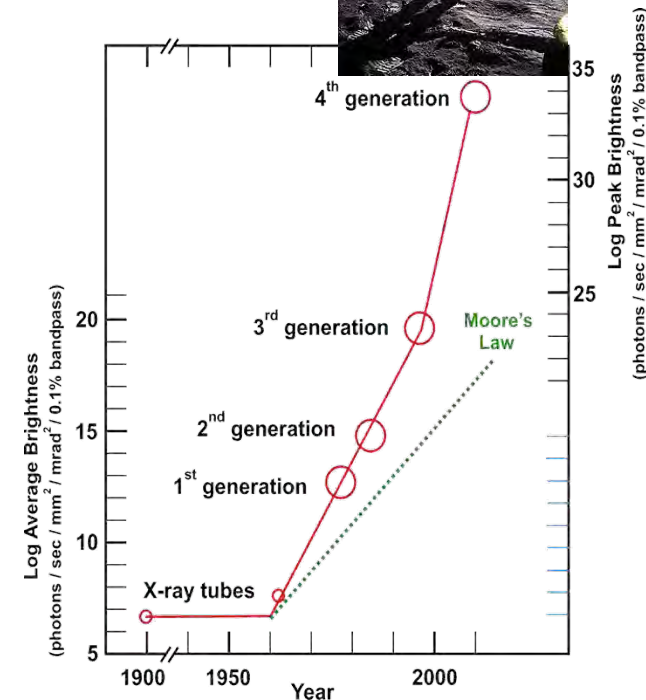
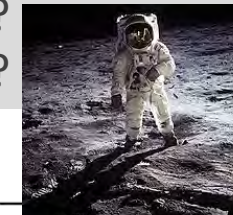
- high harmonic generation
- tabletop coherent x-ray radiation
- attosecond pulses



G. Mourou RMP 2006

High-intensity at x-ray wavelengths

- ?
- ?
- ?



D. Moncton, George Brown



Contrast optical and x-ray interactions at high intensity

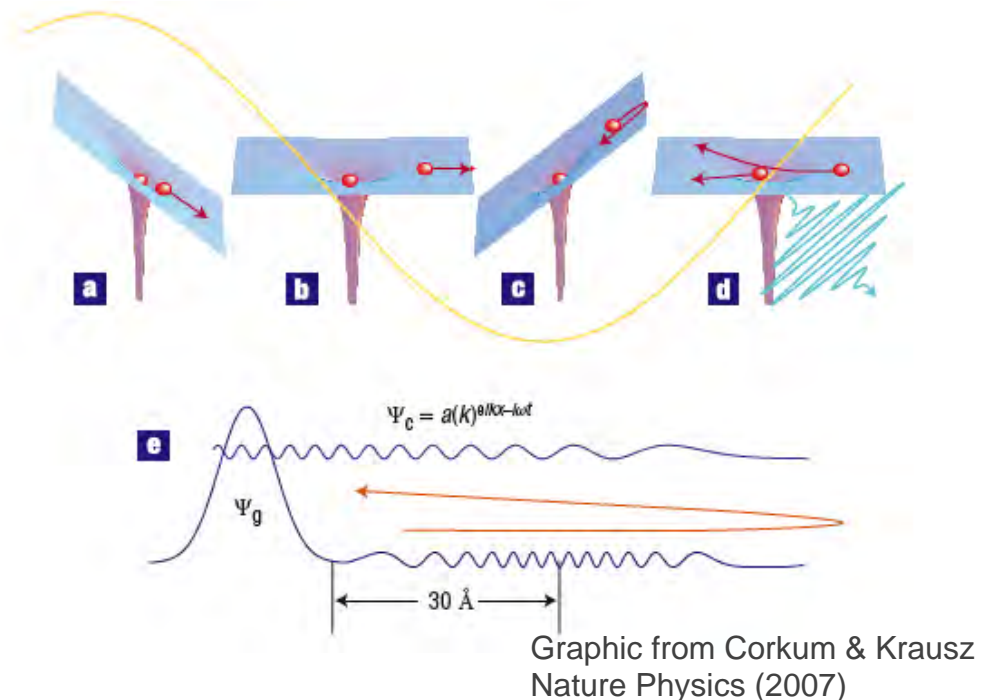
At long wavelengths - laser-driven electron dynamics is dominant
... not so at short wavelengths

electron ponderomotive energy (au)

$$U_p = I/4\omega^2$$

displacement

$$\alpha = E/\omega^2$$



Ti:sapphire laser (1.55 eV) PW/cm²
 $U_p \sim 60 \text{ eV} \text{ & } \alpha \sim 50 \text{ au}$

LCLS (800 eV) 100 PW/cm²
 $U_p \sim 25 \text{ meV} \text{ & } \alpha \sim 0.003 \text{ au}$



Parameters - intense optical lasers vs x-fel

Ti: sapphire

photon energy: 1.5 eV
number of photons: 5×10^{15} /shot
pulse energy: 1 mJ
pulse duration: 30 fs
focused spot size: 1 μm
flux: $5 \times 10^{35} \text{ cm}^{-2} \text{ s}^{-1}$
intensity: 10^{17} W/cm^2

period: 2.7 fs
number of cycles: 10
ponderomotive energy: 6000 eV
displacement: 1000 au

LCLS

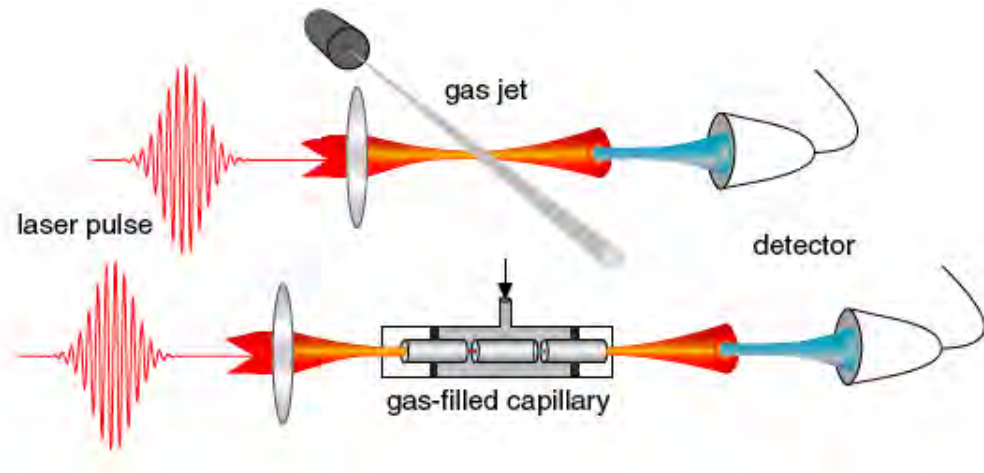
photon energy: 800 eV
number of photons: 10^{13} /shot
pulse energy: 1 mJ
pulse duration: 100 fs
focused spot size: 1 μm
flux: $10^{33} \text{ cm}^{-2} \text{ s}^{-1}$
intensity: 10^{17} W/cm^2

period: 2 as
number of cycles: 40,000
ponderomotive energy: 25 meV
displacement: 0.003 au

Use short pulse optical lasers for extreme nonlinear optics, i.e. generation of high harmonics



High Harmonic Generation: a tabletop ultrafast x-ray source

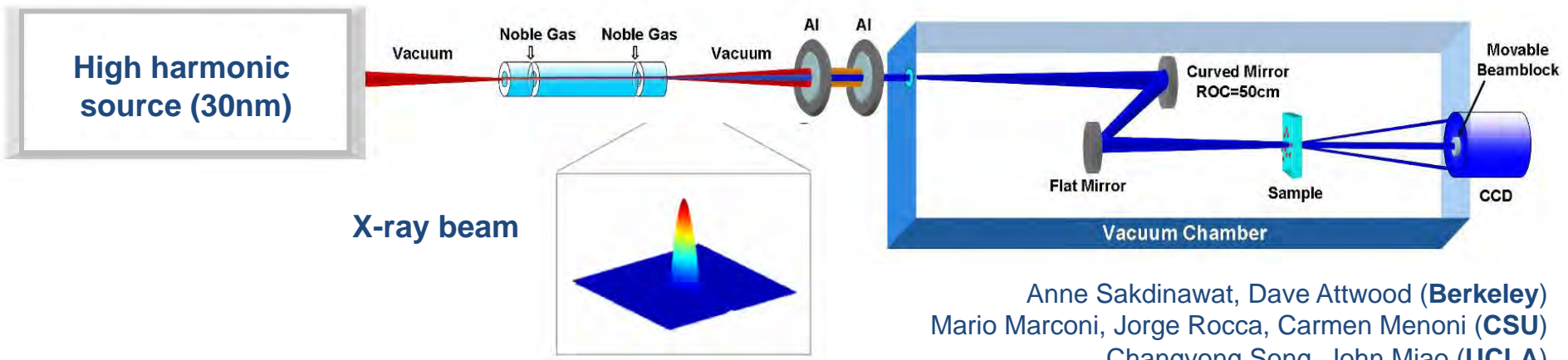


Coherent, collimated, ultrafast (down to attoseconds), tabletop
But - typical conversion efficiency from Ti:sapphire 10^{-5} /harmonic
Frontiers – shorter, more controlled pulses, shorter wavelengths

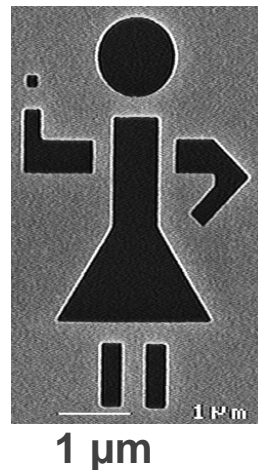
Reviews: T Pfeifer, C Spielmann, G Gerber, Rep Prog Phys (2006)
P Agostini & L DiMauro, Rep Prog Phys (2004)



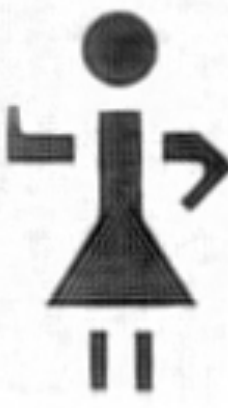
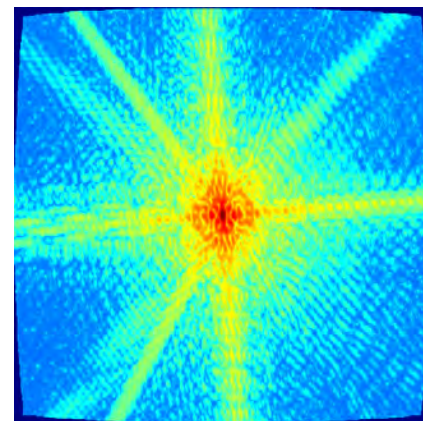
Coherent Diffraction Imaging using HHG beams resolution \approx 90nm



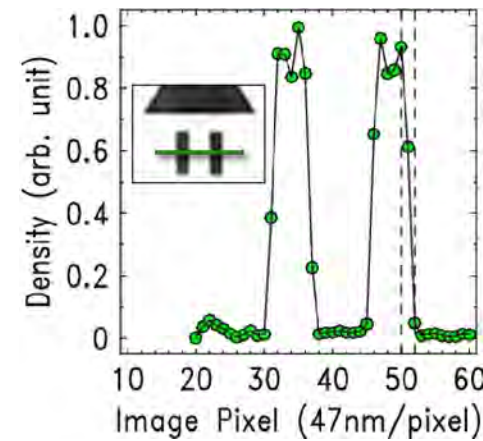
Anne Sakdinawat, Dave Attwood (**Berkeley**)
Mario Marconi, Jorge Rocca, Carmen Menoni (**CSU**)
Changyong Song, John Miao (**UCLA**)
Richard Sandberg, Daisy Raymondson, MM, HK (**JILA**)



sample (SEM image) HHG diffraction pattern



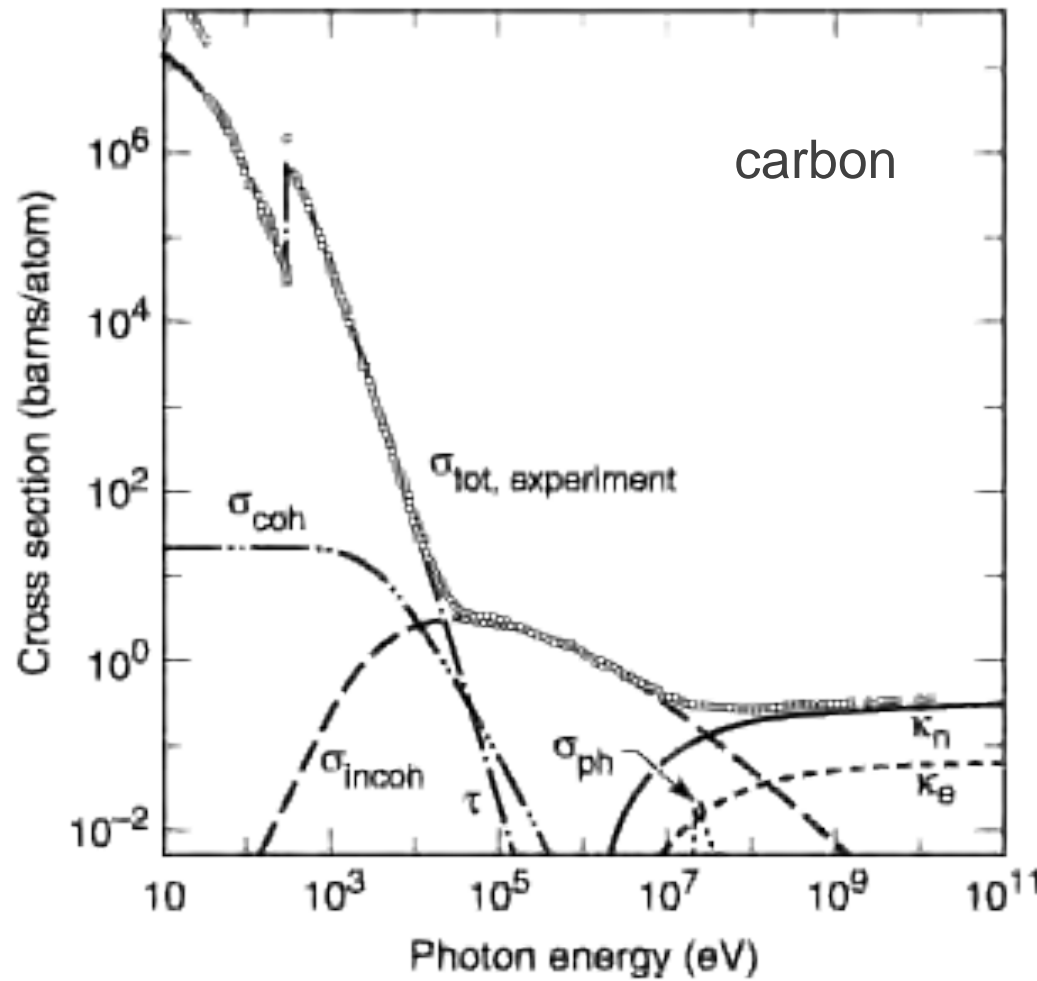
reconstruction



Basic x-ray processes in atoms



Fundamental x-ray atom interactions

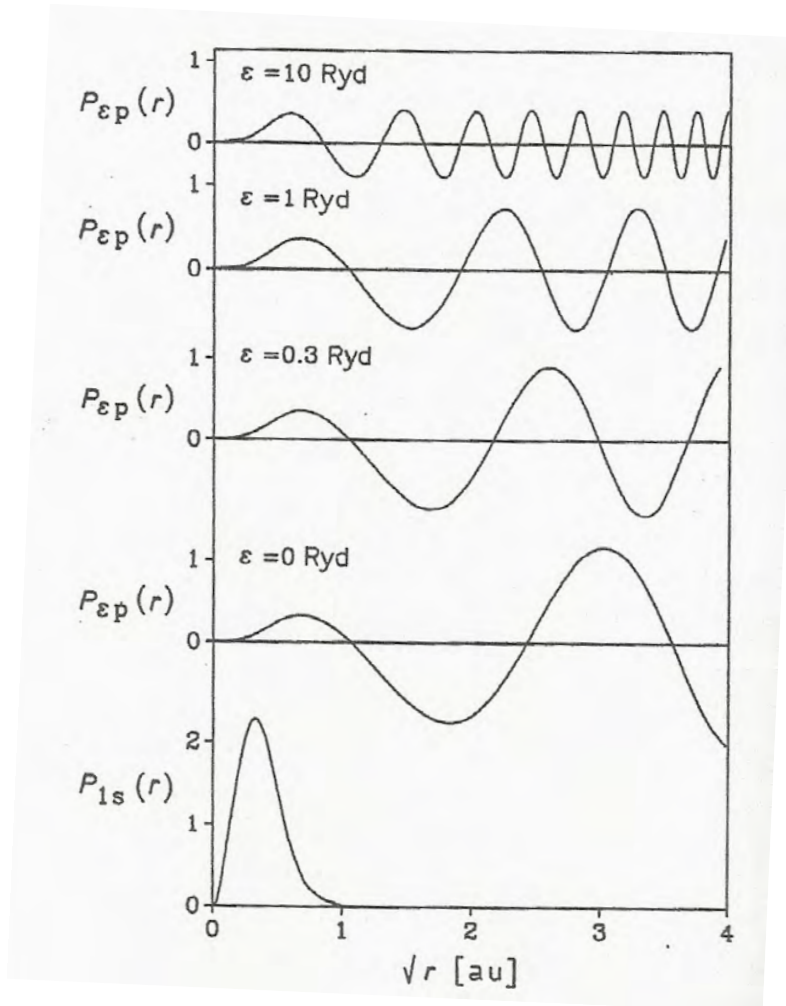


Photoabsorption
Coherent/Rayleigh/Elastic Scattering
Incoherent/Compton Scattering
Pair Production
Photonuclear absorption



Construction of photoionization cross-sections

Radial functions in neon



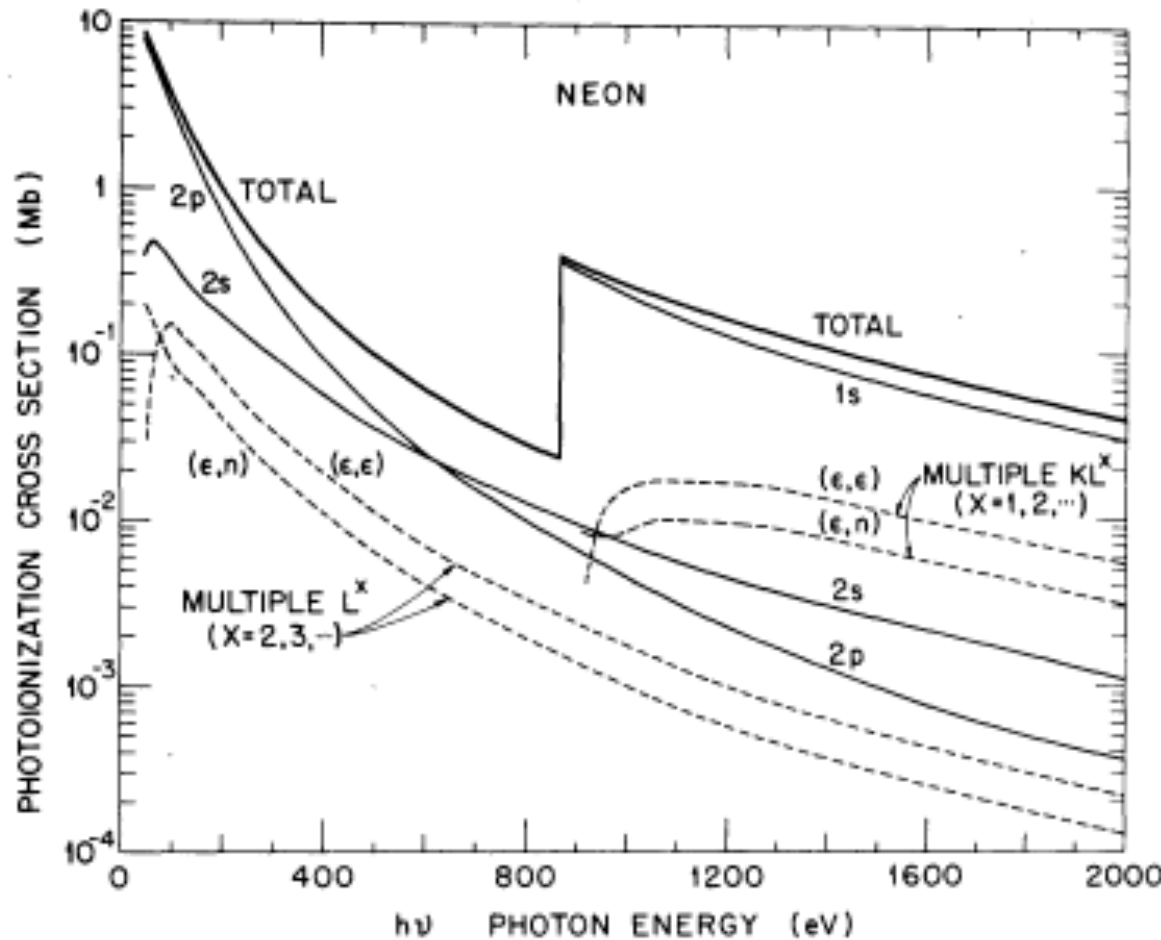
$$\sigma_{1s} = \frac{8\pi^2}{3} \alpha E_{ph} R_{\epsilon p, 1s}^2$$

$$\begin{aligned} R_{\epsilon p, 1s} &= \langle R_{\epsilon p(r)} | r | R_{1s(r)} \rangle \\ &= \int_0^\infty R_{\epsilon p(r)} r R_{1s(r)} r^2 dr \\ &= \int_0^\infty P_{\epsilon p(r)} r P_{1s(r)} dr \end{aligned}$$

$\sigma \propto$ overlap integral weighted by r



Dissection of the total photoabsorption cross section



$$E_{e, \text{kin}}(\epsilon l) = h\nu - E_{nl}$$

$$E_{e, \text{kin}}(\epsilon l, n'l') = h\nu - E_{nl} - E_{n''l'' \rightarrow n'l'}$$

$$E_{e, \text{kin}}(\epsilon l, \epsilon'l') = h\nu - E_{nl} - E_{n''l''} - E_{e, \text{kin}}^*(\epsilon'l', \epsilon l)$$



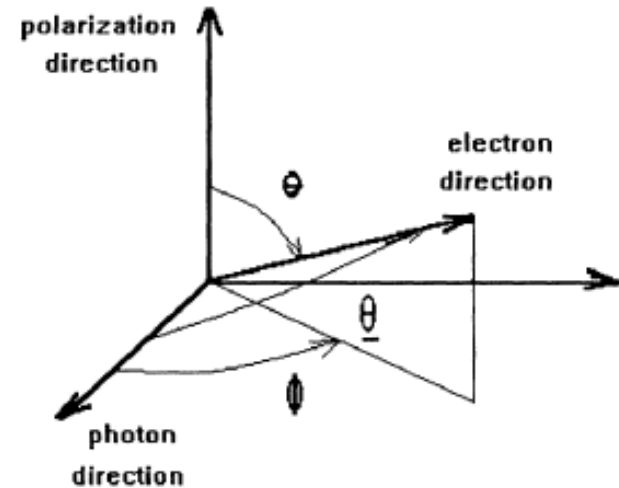
Photoelectron angular distributions

$$\frac{d\sigma}{d\Omega}(\vartheta) = \frac{\sigma}{4\pi} [1 + \beta P_2(\cos(\vartheta))]$$

$$\beta_{1s} = 2$$

$$\beta_{2s} = 2$$

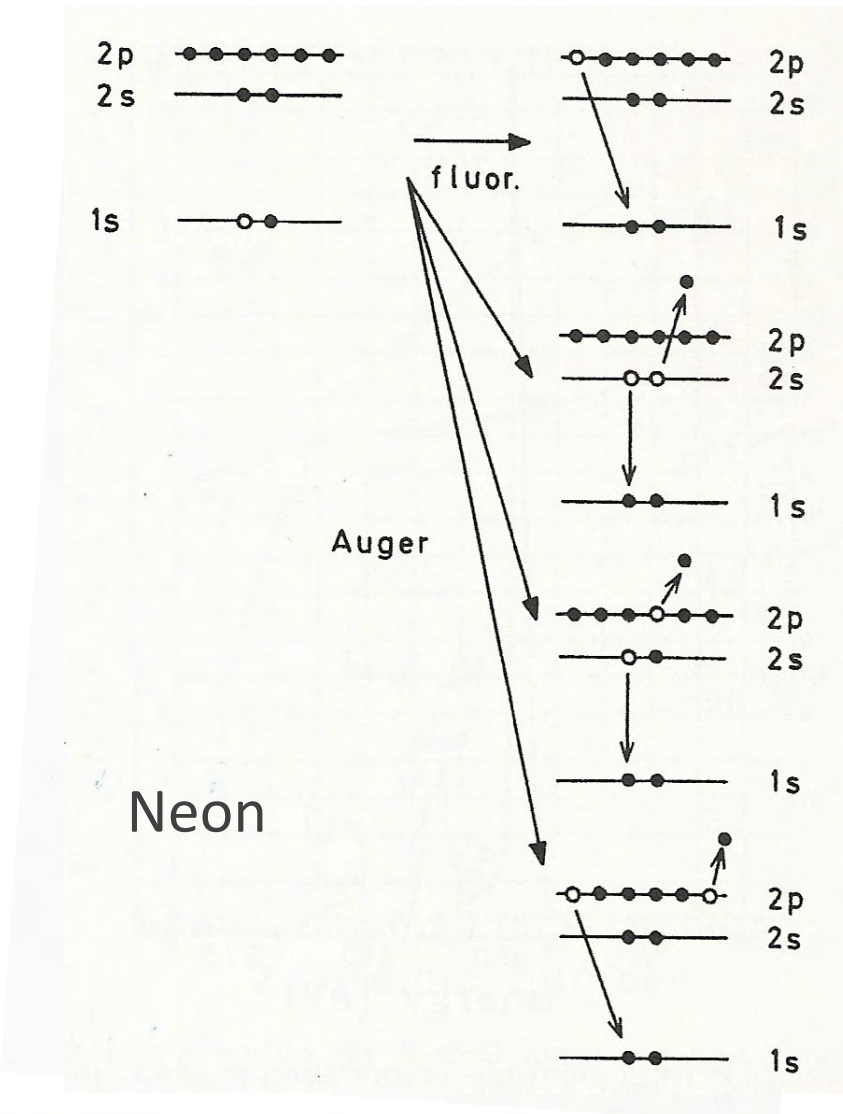
$$\beta_{2p} = \frac{2R_{\epsilon d, 2p}^2 - 4R_{\epsilon d, 2p}R_{\epsilon s, 2p} \cos(\Delta)}{R_{\epsilon s, 2p}^2 + 2R_{\epsilon d, 2p}^2}$$



Angle independent measure of cross section at “magic” angle 54.7° where $P_2 \cos(\theta) = 0$.



What's after photoabsorption (1s hole creation)?



Radiative – fluorescence

Operator: dipole

Selection Rules

$$\Delta J = \pm 1, 0, J = 0 \rightarrow J = 0 \text{ forbidden}$$

Parity change

Non-radiative – Auger

Operator: Coulomb interaction

$$Op(Auger) = \sum_{i < j} \frac{1}{r_{ij}}$$

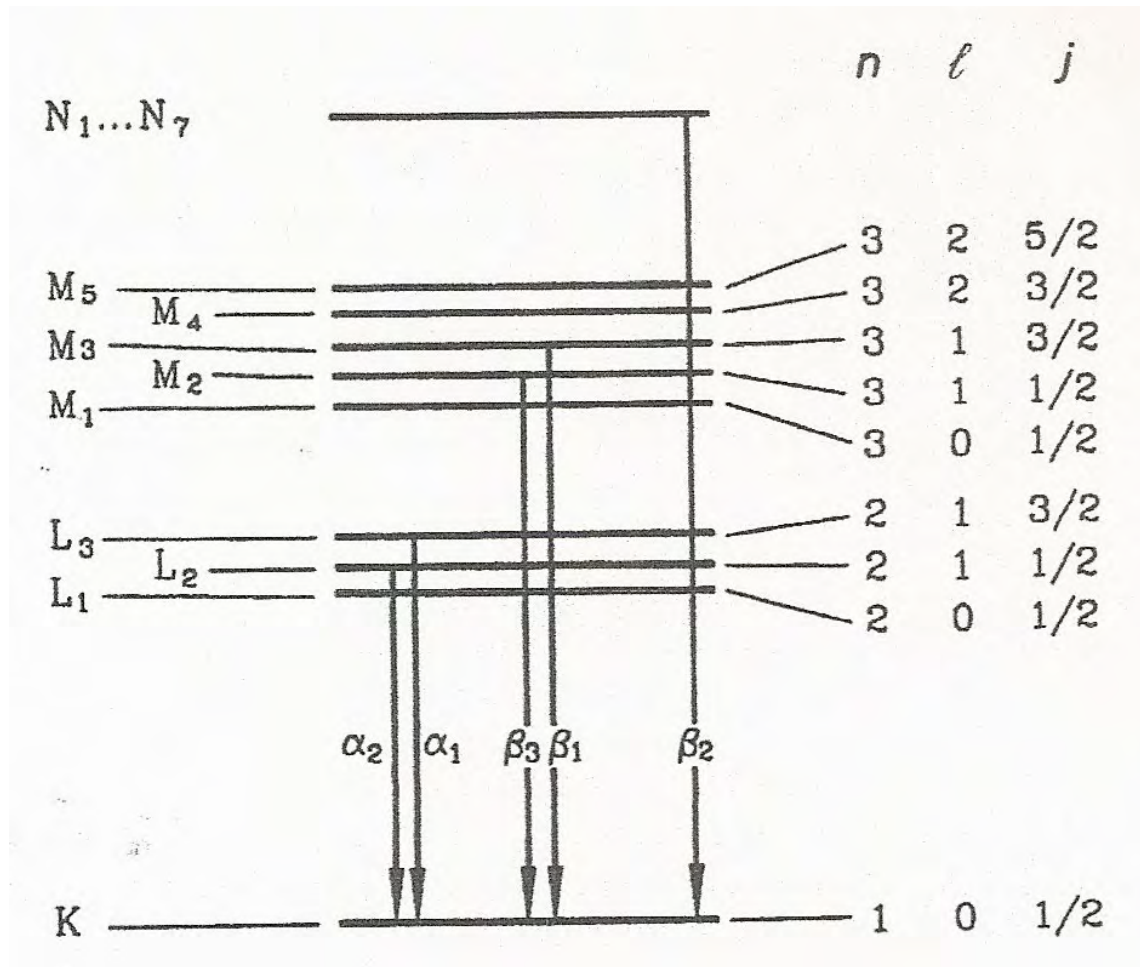
Selection Rules

$$\Delta L = \Delta S = \Delta M_L = \Delta M_S = 0$$

No parity change



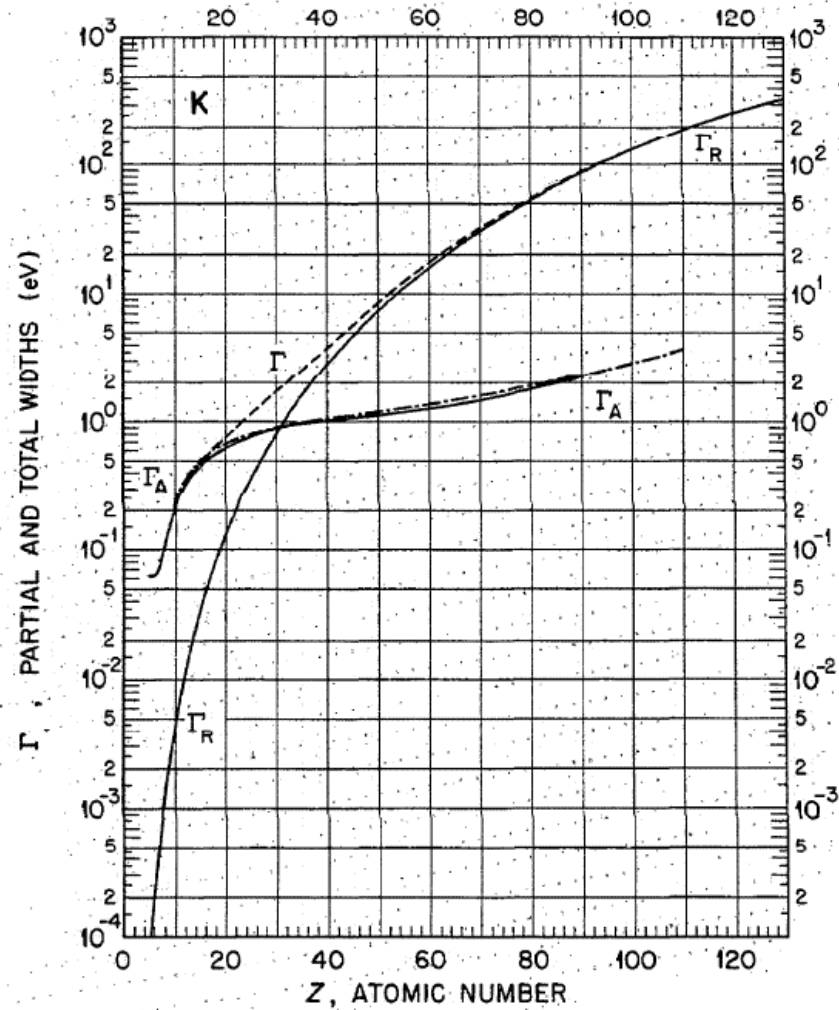
Nomenclature for inner-shell transitions



For example: Auger lines labelled $K-L_{2,3}L_{2,3}$, $K-L_{2,3},L_1$, $K-L_1L_1$
Hollow atoms: $KK-KL_{2,3}L_{2,3}\dots$



Relative probability for radiative and Auger decay



$$\Gamma\tau = \hbar$$

$$\Gamma(1s) = \Gamma_R(1s) + \Gamma_A(1s)$$

$$(\hbar = 0.657 eV fs)$$

Z-dependence

$$\gamma_R = \frac{4\omega_0^3}{3\hbar c^3} \frac{|\langle g, J || r || e, J' \rangle|^2}{2J' + 1}$$

$$\omega_0 \propto Z^2, \langle r \rangle \propto 1/Z \implies \gamma_R \propto Z^4$$

M. O. Krause, JPCRD (1979)



Ab initio calculations of Auger rates

Neon K-LL transition
5 lines: Initial state = [1s 2s²2p⁶] = ²S^e

Ne ²⁺ channel	Auger-electron energy	Relative Auger intensity
2p ⁻² ¹ D ^e	804	10.1
2p ⁻² ¹ S ^e	800	1.5
2s ⁻¹ 2p ⁻¹ ³ P ^o	782	1.1
2s ⁻¹ 2p ⁻¹ ¹ P ^o	771	2.9
2s ⁻² ¹ S ^e	748	1.0

H. Kelly, Phys Rev A **11**, 556 (1975) Hartree Fock + correlation

Ne neutral

C. Bhalla et al., Phys Rev A **8**, 649 (1973) Hartree-Fock-Slater (+ configuration mixing)

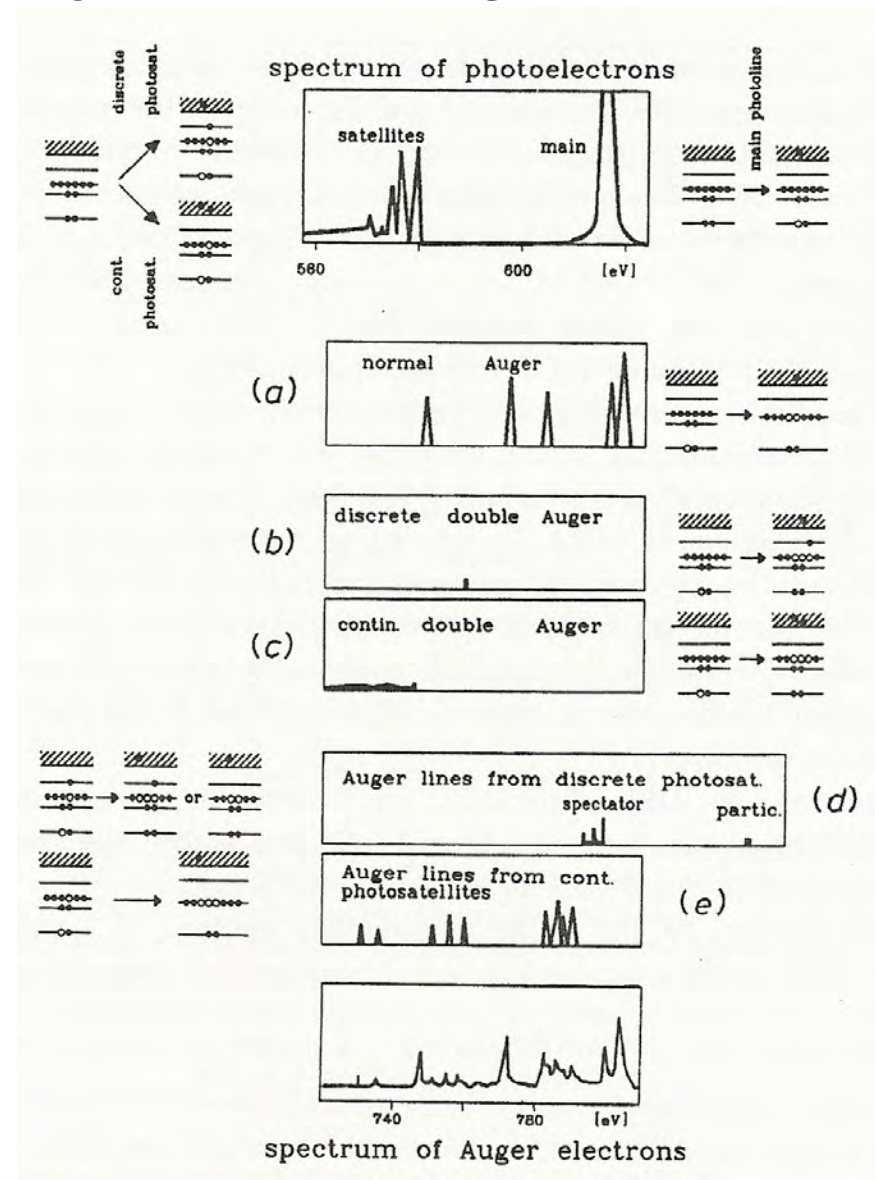
All charge states & configurations

M.H. Chen, Phys Rev A **44**, 239 (1991) Multiconfiguration Dirac Fock
[KK] energies and radiative & Auger transition rates vs Z

New toolkit: Sang-Kil Son & Robin Santra, Phys Rev A (2011) Hartree-Fock-Slater framework



Beyond the diagram lines: Example neon



From V. Schmidt

Categories of Auger lines

A: normal Auger from 1s photoionization

B α & B β : satellite lines from 1s – nl excitations with spectator or participator transition

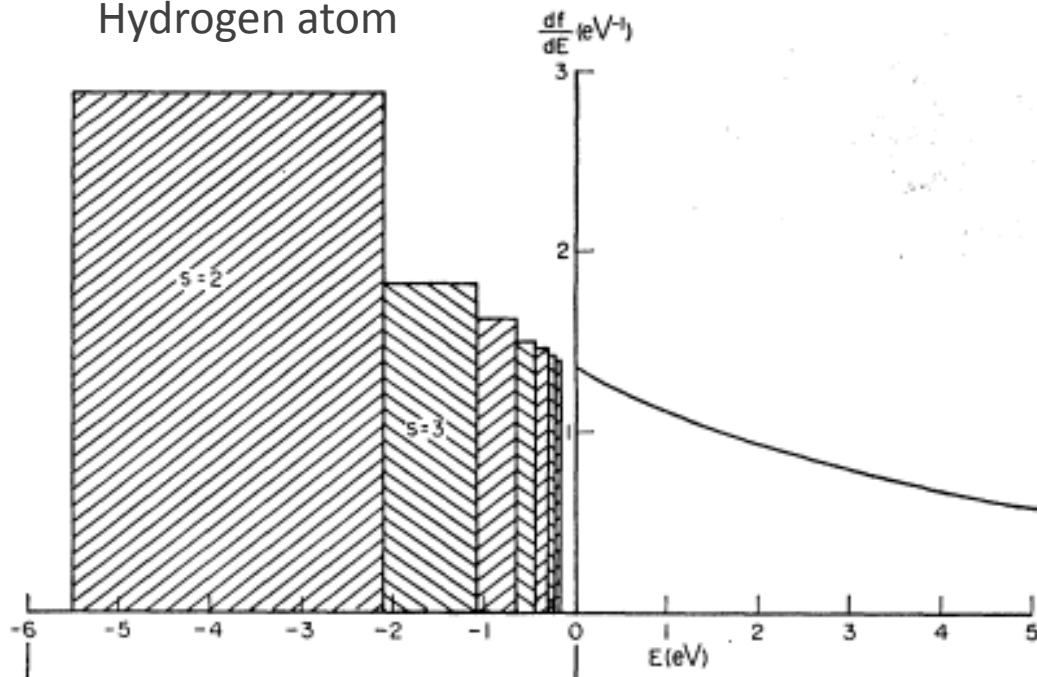
C α & C β : KL* - LLL* arising from 1s, 2s- ∞ , nl and 1s, 2p – ∞ , nl two electron processes of ionization and excitation with subsequent Auger decay where excited electron is involved or spectating

D: KL – LLL Auger transitions from 1s, 2s – ∞ , ∞ and 1s, 2p – ∞ , ∞ two electron processes with subsequent Auger decay



Distribution of absorption oscillator strength

Hydrogen atom



Fano & Cooper, RMP (1968)

Smooth transition: discrete to continuum

Discrete transitions:
Area = average oscillator strength

$$\bar{f}_{n'l',nl} = \frac{2}{3} \omega_{n'l',nl} \frac{l_{max}}{2l+1} |\langle n, l | r | n'l' \rangle|^2$$

$$\int_0^\omega \sigma(\omega) d\omega = 2\pi^2 r_0 c f_{ik}$$

Continuum

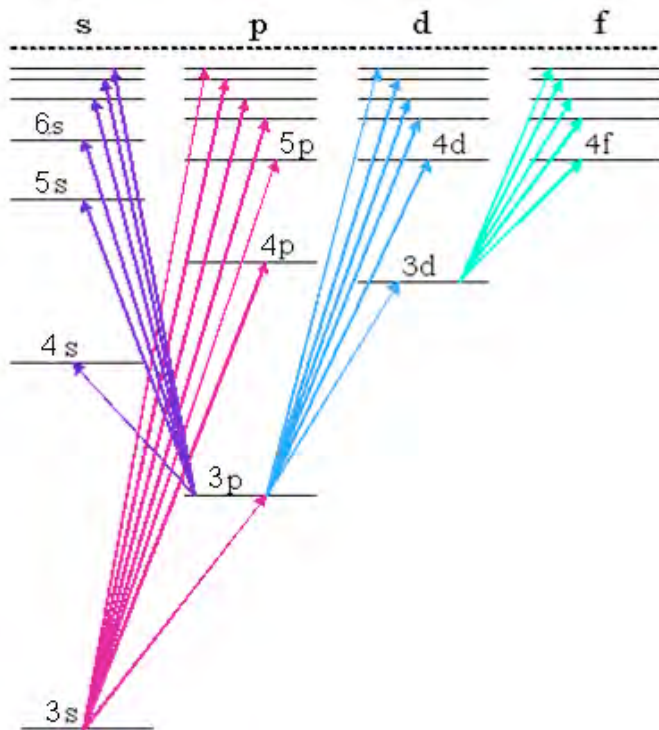
$$\frac{d\bar{f}_{\epsilon'l',nl}}{dW} = \frac{2}{3} \omega_{\epsilon'l',nl} \frac{l_{max}}{2l+1} |\langle \epsilon'l' | r | nl \rangle|^2$$

$$\sigma = \frac{2\pi^2}{c} \cdot \frac{d\bar{f}_{\epsilon'l',nl}}{cdW}$$



An aside - bound-bound transitions & laser cooling

Grotian Diagram for Sodium



Energy levels & oscillator strengths involved in laser cooling of sodium

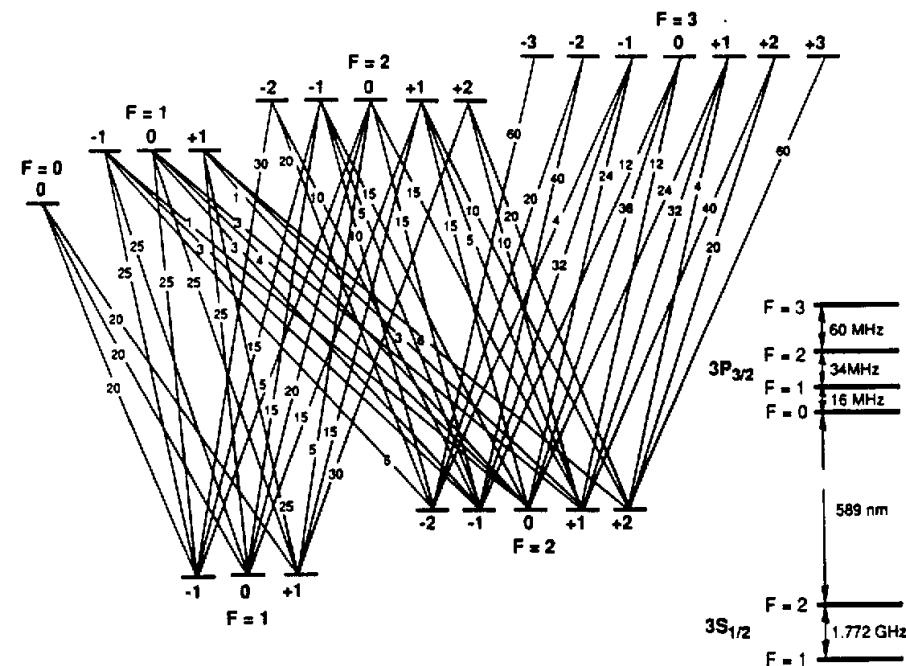


Fig. 2.2: Oscillator strengths and energy separations for the sodium $3S_{1/2} \rightarrow 3P_{3/2}$ hyperfine transitions.



Scattering factors & refractive index & susceptibility can be derived from absorption cross sections

$$f(E) = f_1(E) + i f_2(E)$$

$$f_1(E) = Z + C \int_0^{\infty} \frac{\epsilon^2 \mu_a(\epsilon) d\epsilon}{E^2 - \epsilon^2}$$

$$f_2(E) = \frac{\pi}{2} C E \mu_a(E) \quad \text{where } C = 1/\pi r_0 h c$$

$$n = 1 - \delta - i\beta = \sqrt{1 + 4\pi\chi} \approx 1 + 2\pi\chi = 1 + 2\pi N\alpha$$

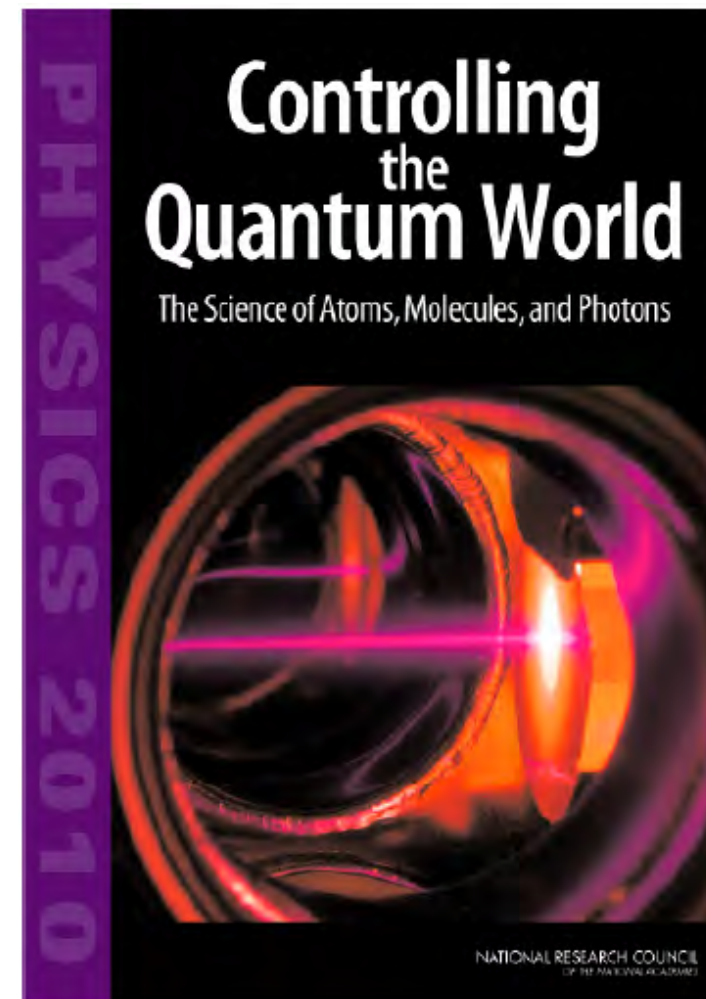
$$\delta = K f_1, \beta = K f_2 \text{ where } K = \frac{r_0 \lambda^2}{2\pi} \frac{N_A}{A} \rho$$





Optical control of x-ray processes



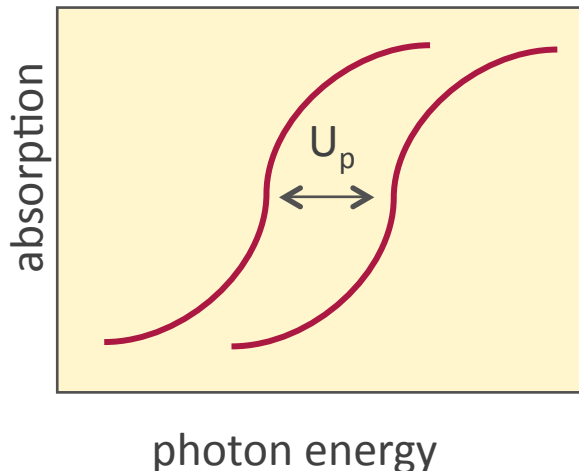


Modification of x-ray processes by strong optical fields

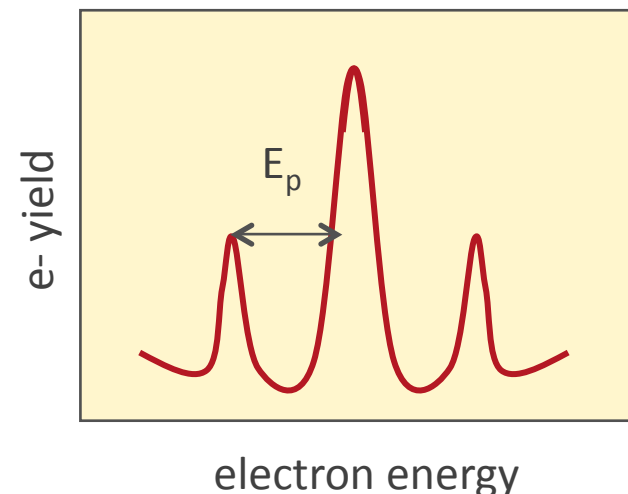
Motivations

- Understand changes to x-ray processes in presence of strong laser fields
- Theoretical predictions
 - ponderomotive shift in threshold \Rightarrow absorption spectrum
 - free-free transitions in continuum \Rightarrow electron spectra

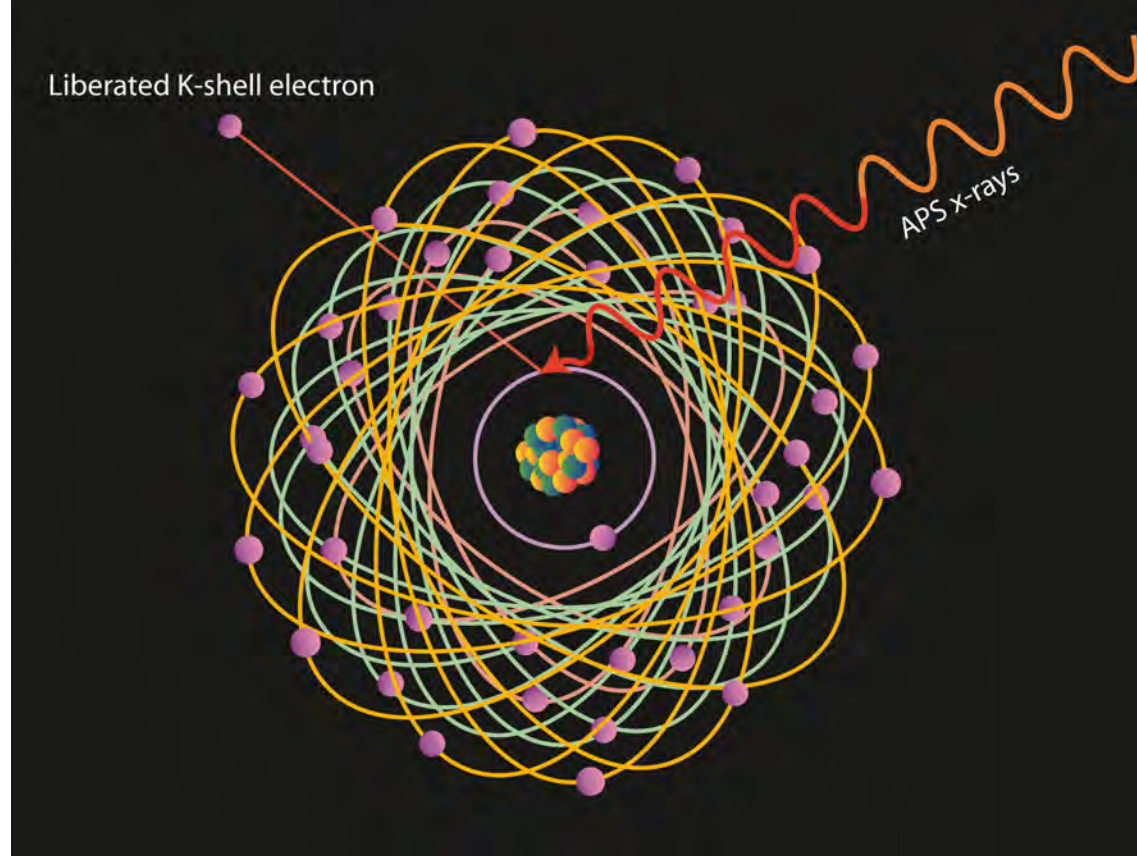
Ponderomotive shift



Electron satellites



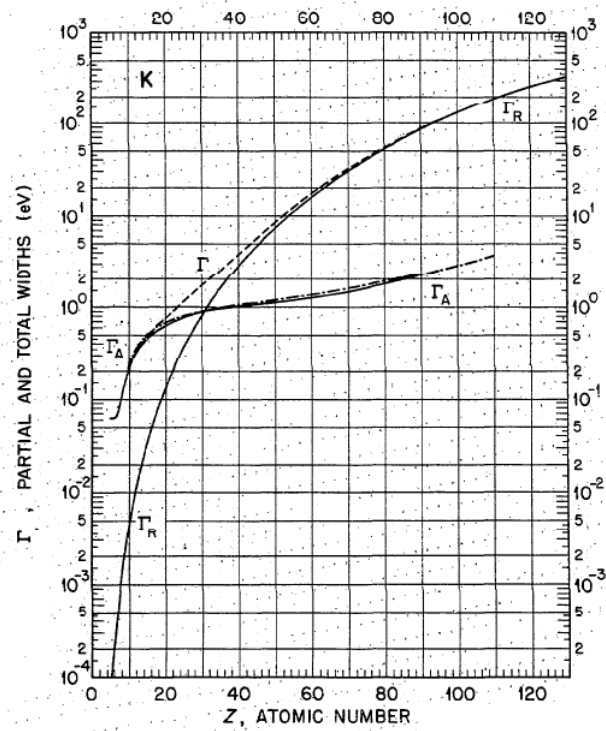
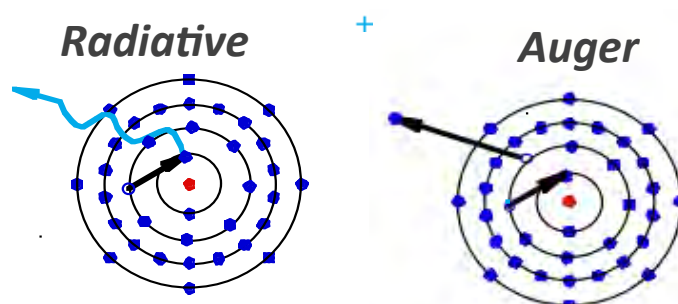
Can strong optical fields control x-ray processes?



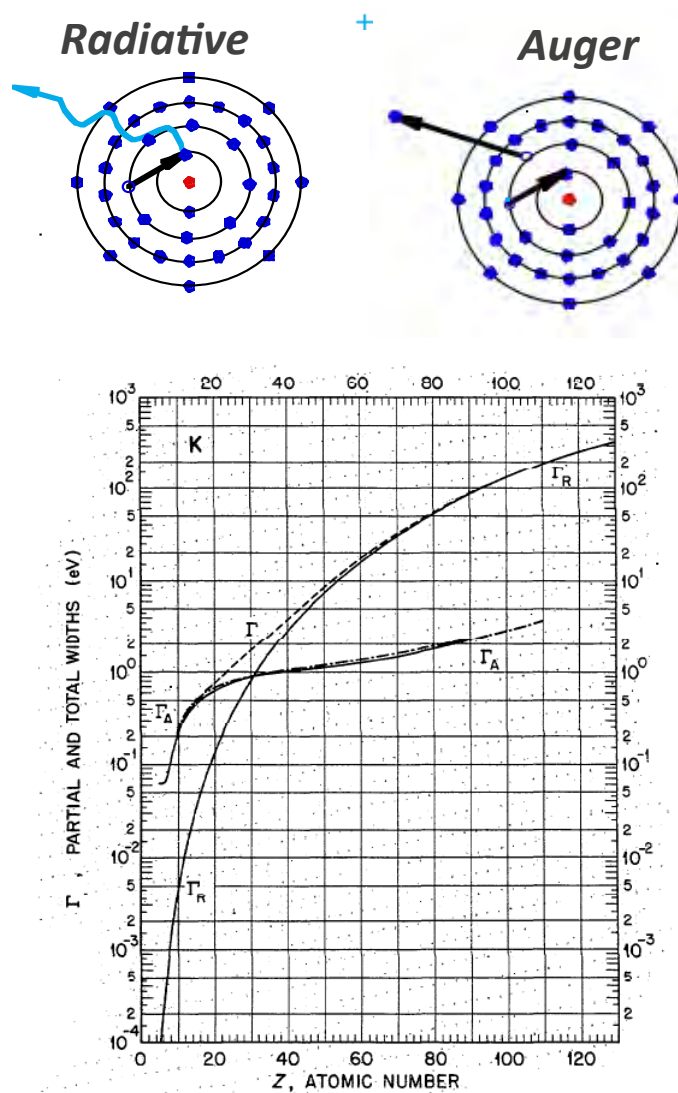
- *Optical laser-induced processes must compete with inner-shell decay*
- *Typical inner shell decay width 1eV \Rightarrow 0.66 fs lifetime*



Intraatomic inner-shell decay vs laser-driven transitions

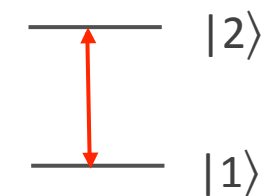


Intraatomic inner-shell decay vs laser-driven transitions



Rabi frequency

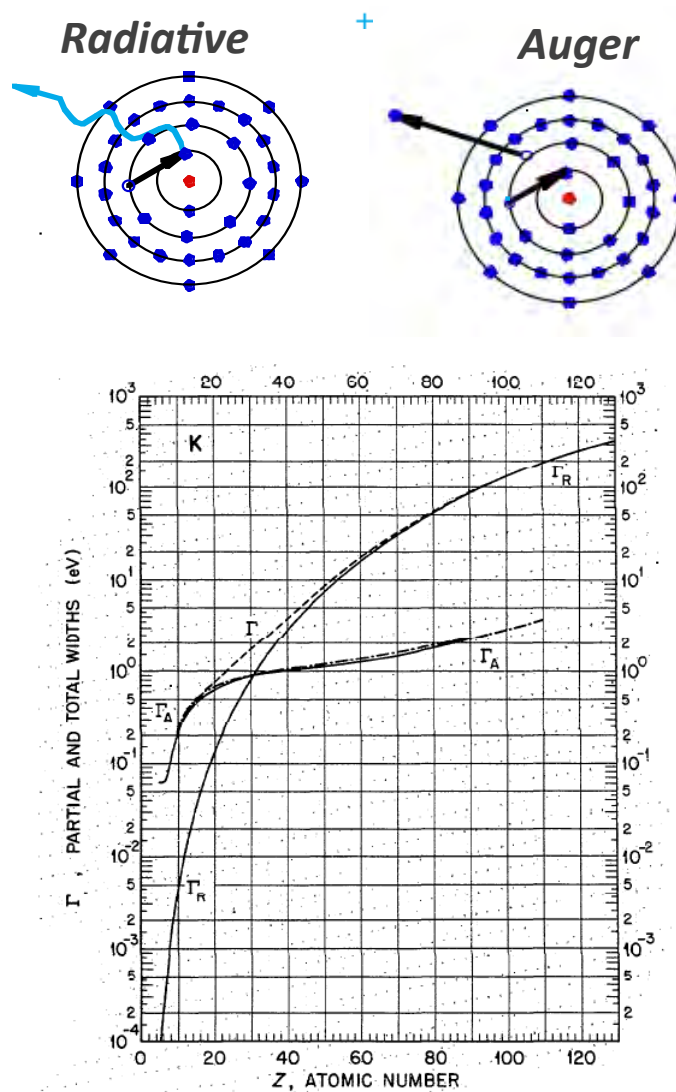
$$\Omega_{12} = \frac{\mu_{12} E}{\hbar}$$



$$\mu = er$$

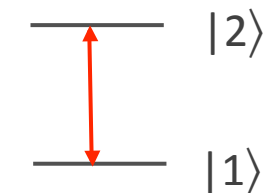


Intraatomic inner-shell decay vs laser-driven transitions



Rabi frequency

$$\Omega_{12} = \frac{\mu_{12} E}{\hbar}$$



$$\mu = er$$

$$\mu_{H1s-2p1/2} = 1.05 \text{ } ea_0$$

Atomic Units : Hydrogen

Charge: electron charge = e

Length: Bohr radius $a_0 = 0.529 \text{ \AA}$

Velocity: Bohr velocity $\alpha c = 1/137 c$

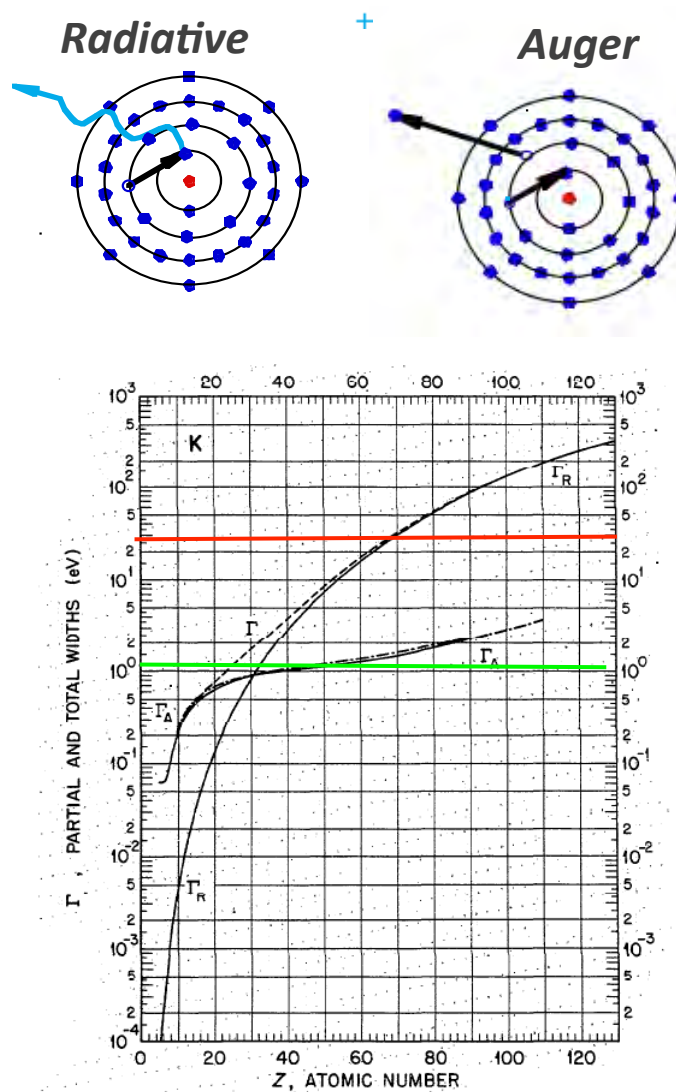
Time: length/velocity = 0.024 fs

Electric field: field at Bohr radius = 51 V/\AA

Intensity: $3.5 \times 10^{16} \text{ W/cm}^2$

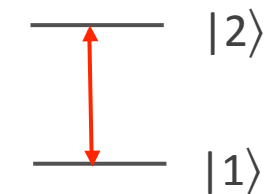


Intraatomic inner-shell decay vs laser-driven transitions



Rabi frequency

$$\Omega_{12} = \frac{\mu_{12} E}{\hbar}$$



$$\mu = er$$

$$\mu_{H1s-2p1/2} = 1.05 \text{ } ea_0$$

Atomic Units : Hydrogen

Charge: electron charge = e

Length: Bohr radius $a_0 = 0.529 \text{ \AA}$

Velocity: Bohr velocity $\alpha c = 1/137 c$

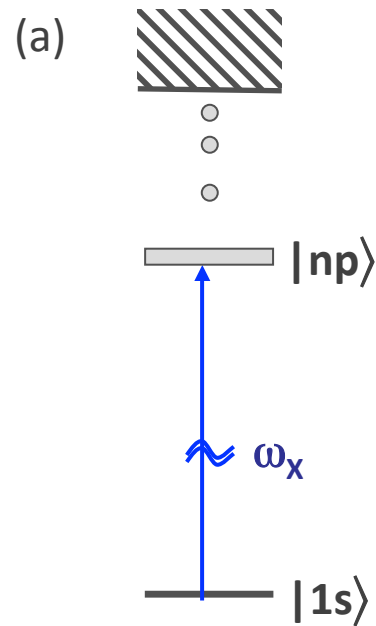
Time: length/velocity = 0.024 fs

Electric field: field at Bohr radius = 51 V/\AA

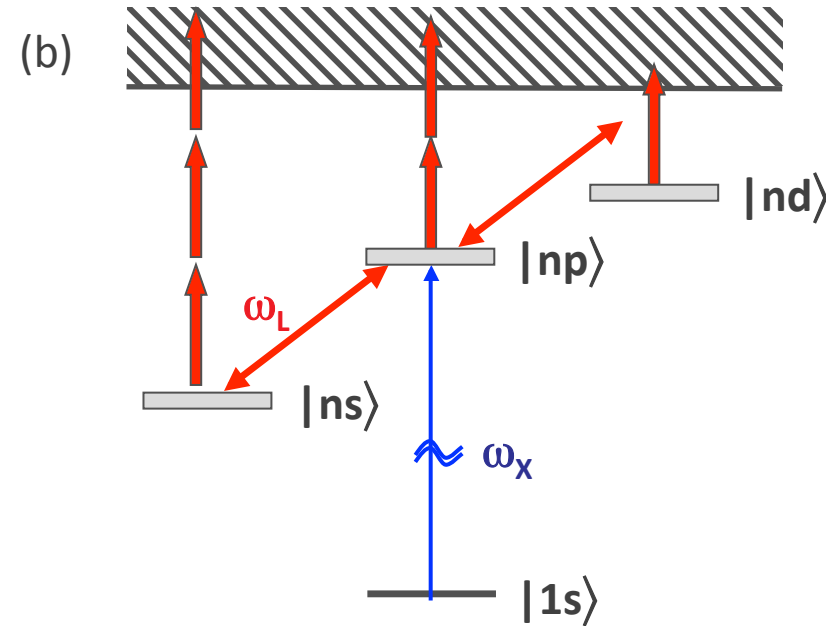
Intensity: $3.5 \times 10^{16} \text{ W/cm}^2$



High intensity laser dressing of core-excited states



Laser-free



With strong-coupling laser



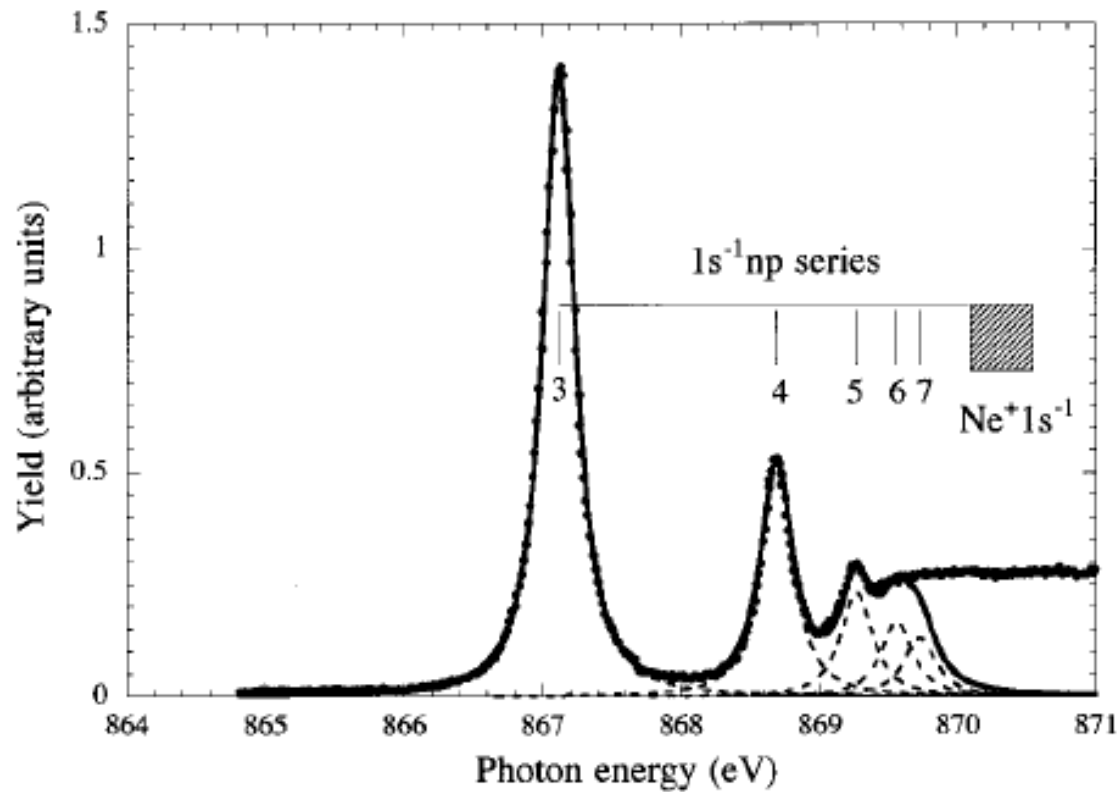


Control of x-ray absorption in neon

Ultrafast, reversible x-ray switch



Choice of neon



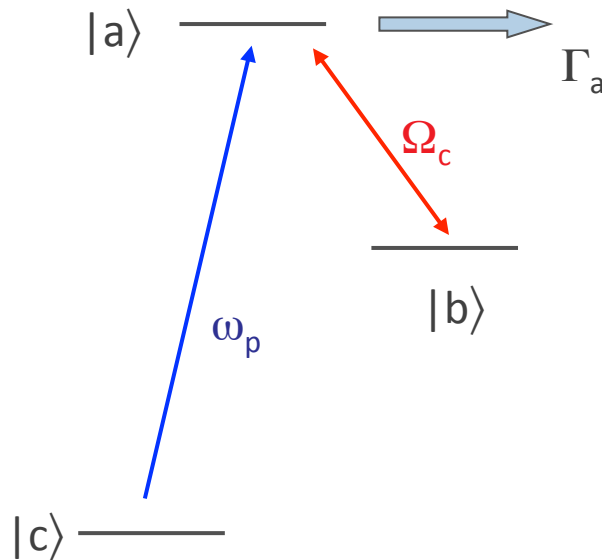
- Isolated resonance
- High IP = 21.6 eV



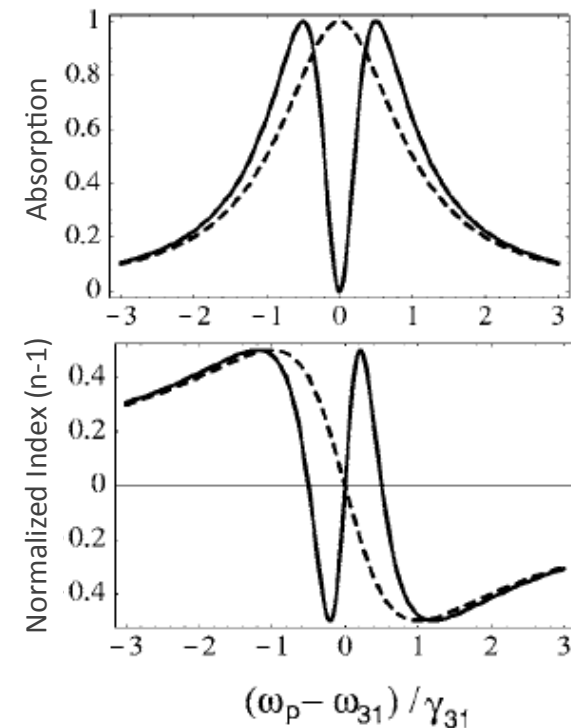
Electromagnetically Induced Transparency (EIT)

*One can make opaque resonant transitions
transparent to laser radiation ...*

- S.E. Harris



$$v_{gr} = \frac{c}{n + \omega_p (dn/d\omega_p)}$$



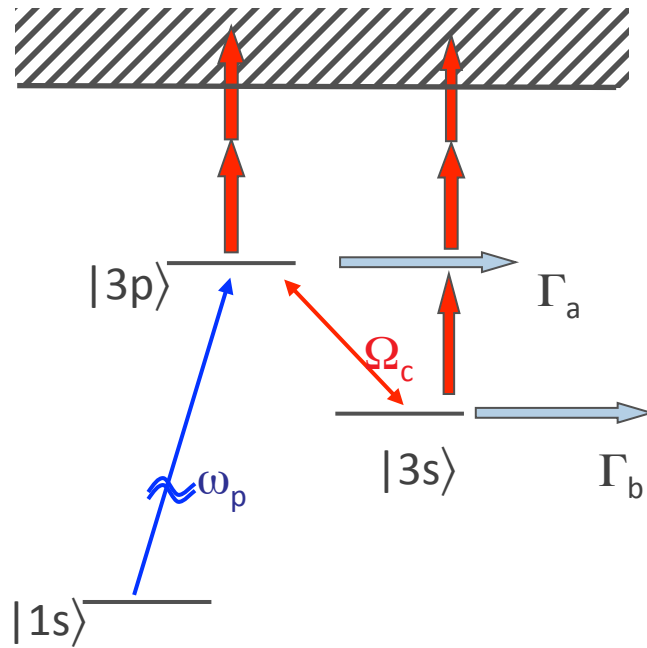
**Light speed reduction
to 17 metres per second
in an ultracold atomic gas**

Lene Vestergaard Hau^{*†}, S. E. Harris[†], Zachary Dutton^{*†}
& Cyrus H. Behroozi[§]

Nature 397, 594 (1999)



Extend EIT concept to soft x-ray regime: Neon



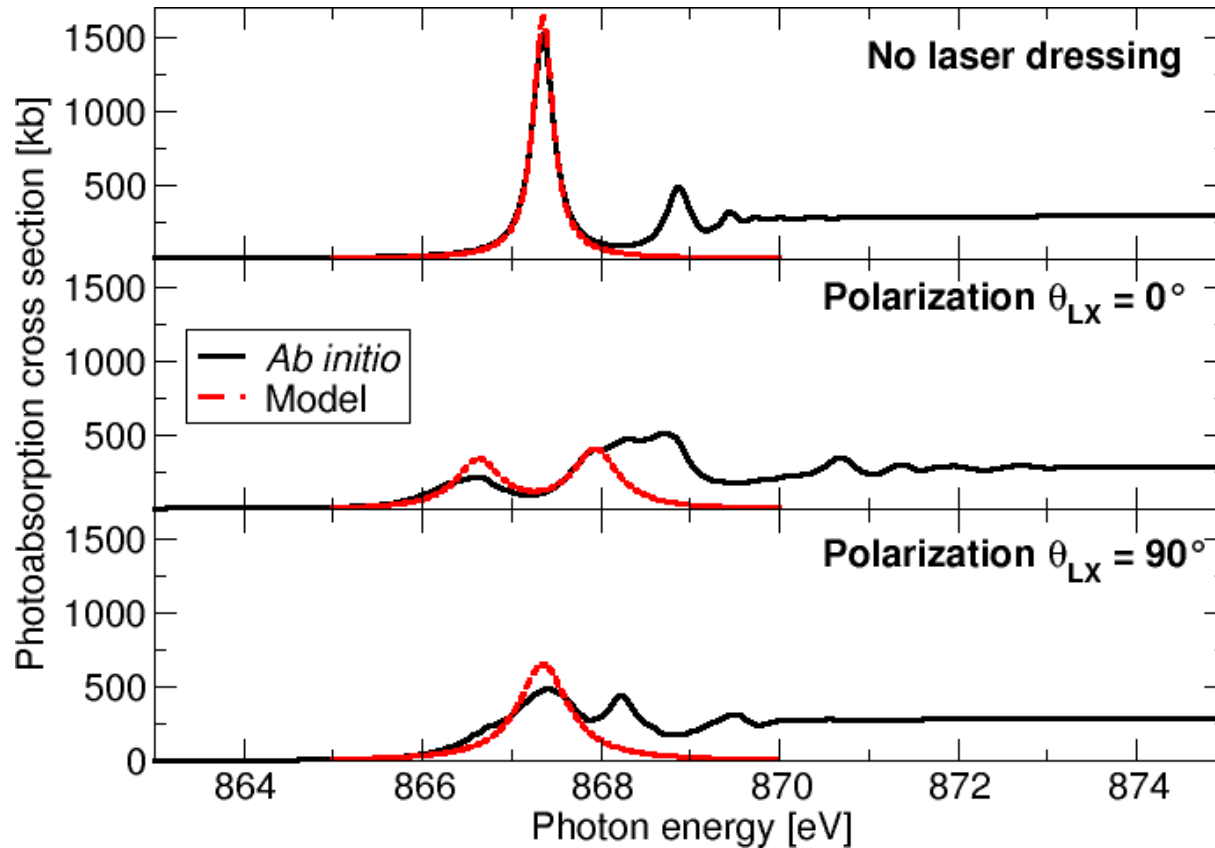
Neon
 $\Gamma_{1s} \sim 0.27 \text{ eV}$
 $\Delta_{3s-3p} = 1.88 \text{ eV}$

Complexities

- Rapid Auger decay (2.4 fs)
- Laser induced ionization of core-excited states
- Existence of resonances at requisite coupling intensity
- $\tau_{\text{Auger}} \sim \tau_{\text{Rabi}} \sim \tau_{\text{Laser}}$



Extend EIT concept to soft x-ray regime: Neon



Laser dressing intensity
 10^{13} W/cm^2
 $800 \text{ nm}(1.55 \text{ eV})$

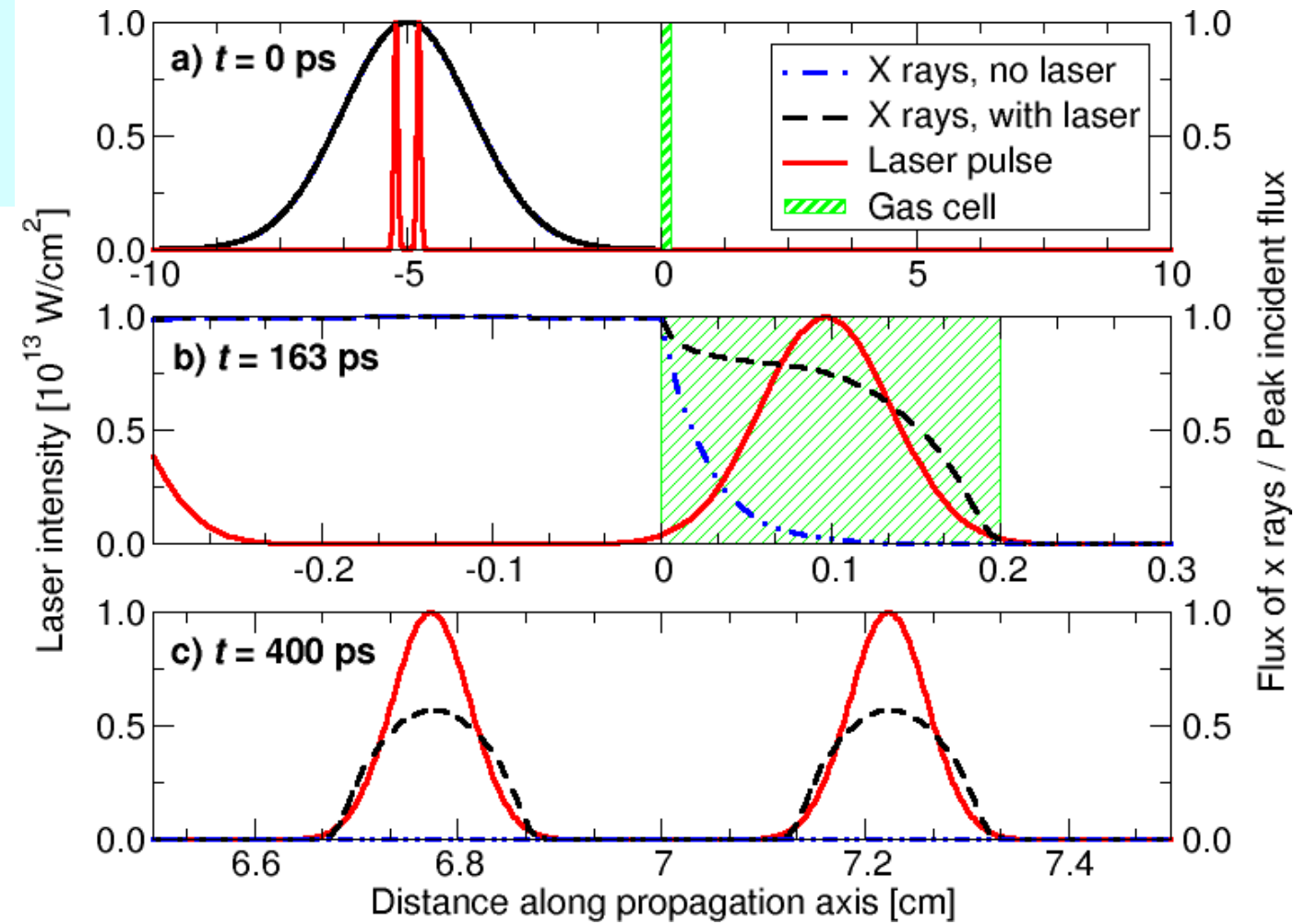
$1 \text{ mJ}/100\text{fs}/(300\mu\text{m})^2$

$$\frac{\sigma(\omega_X, 0^\circ)}{\sigma_0} = \frac{4\Gamma_a^2\Delta_{LX}^2 + \Gamma_a\Gamma_b(\Omega_{ab}^2 + \Gamma_a\Gamma_b)}{[\Omega_{ab}^2 + \Gamma_a\Gamma_b - 4\Delta_{LX}(\omega_{ac} - \omega_X)]^2 + 4[\Gamma_a\Delta_{LX} + \Gamma_b(\omega_{ac} - \omega_X)]^2}.$$



Imprinting ultrafast laser pulse sequences on long x-ray pulses

1 atm Ne, 2-mm
 10^{13} W/cm^2 @ 800 nm
 $T_{\text{No Laser}} = 0.07\%$
 $T_{\text{Laser}} = 57\%$



Exptl demonstration: Controlling x-rays with light



Femtosecond slicing beamline at Advanced Light Source

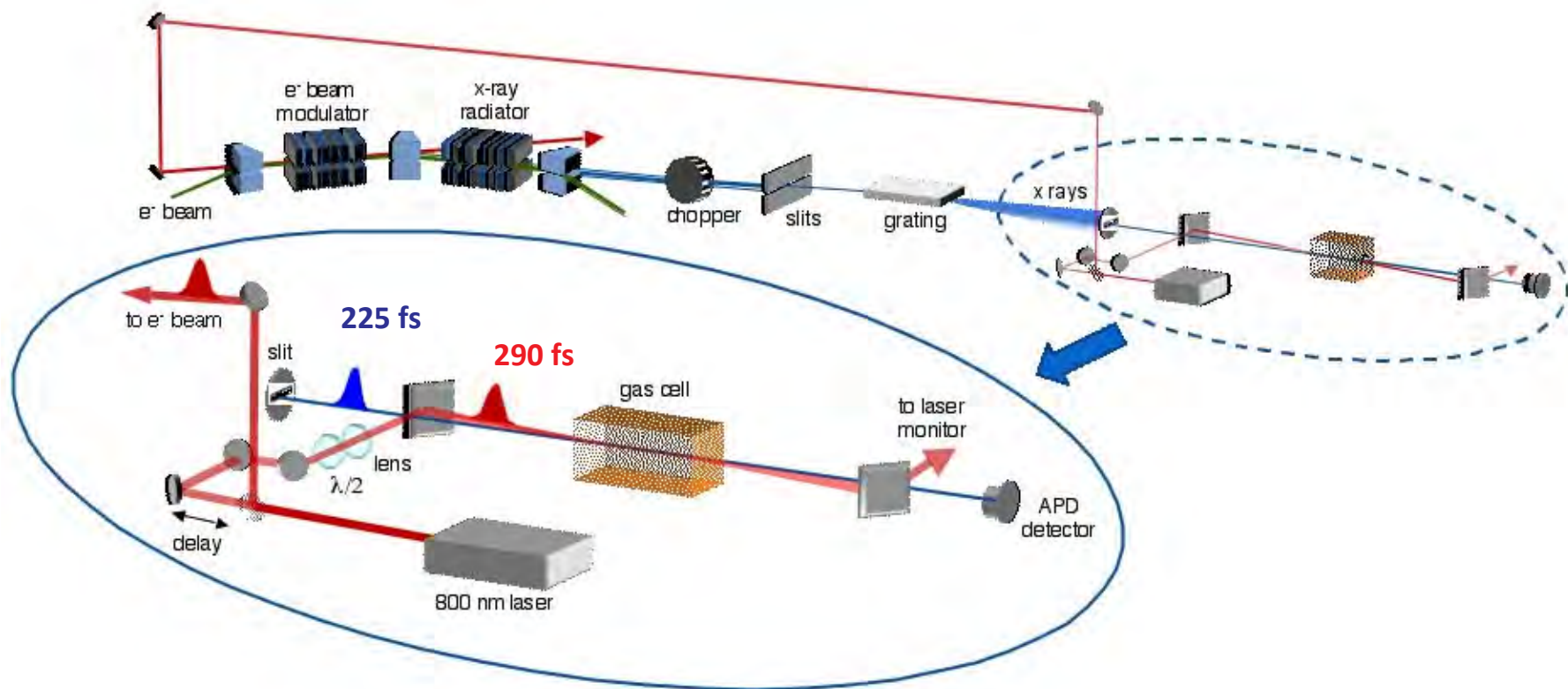
Co-located dressing laser (10^{13} W/cm 2) &
Monochromatic, tunable, short pulse (200 fs) soft x-rays (~870 eV)

Berkeley: T.E. Glover, M. Hertlein, T. Allison, J. van Tilborg, A. Belkacem, B. Rude

Argonne: E.P. Kanter, B. Krässig, R. Sanra, S.H. Southworth, H.R. Varma, L. Young



ALS Femtosecond Spectroscopy Beamline & gas phase transient absorption apparatus



In situ characterization

Starting overlap: ~3 ps, ~2 microns

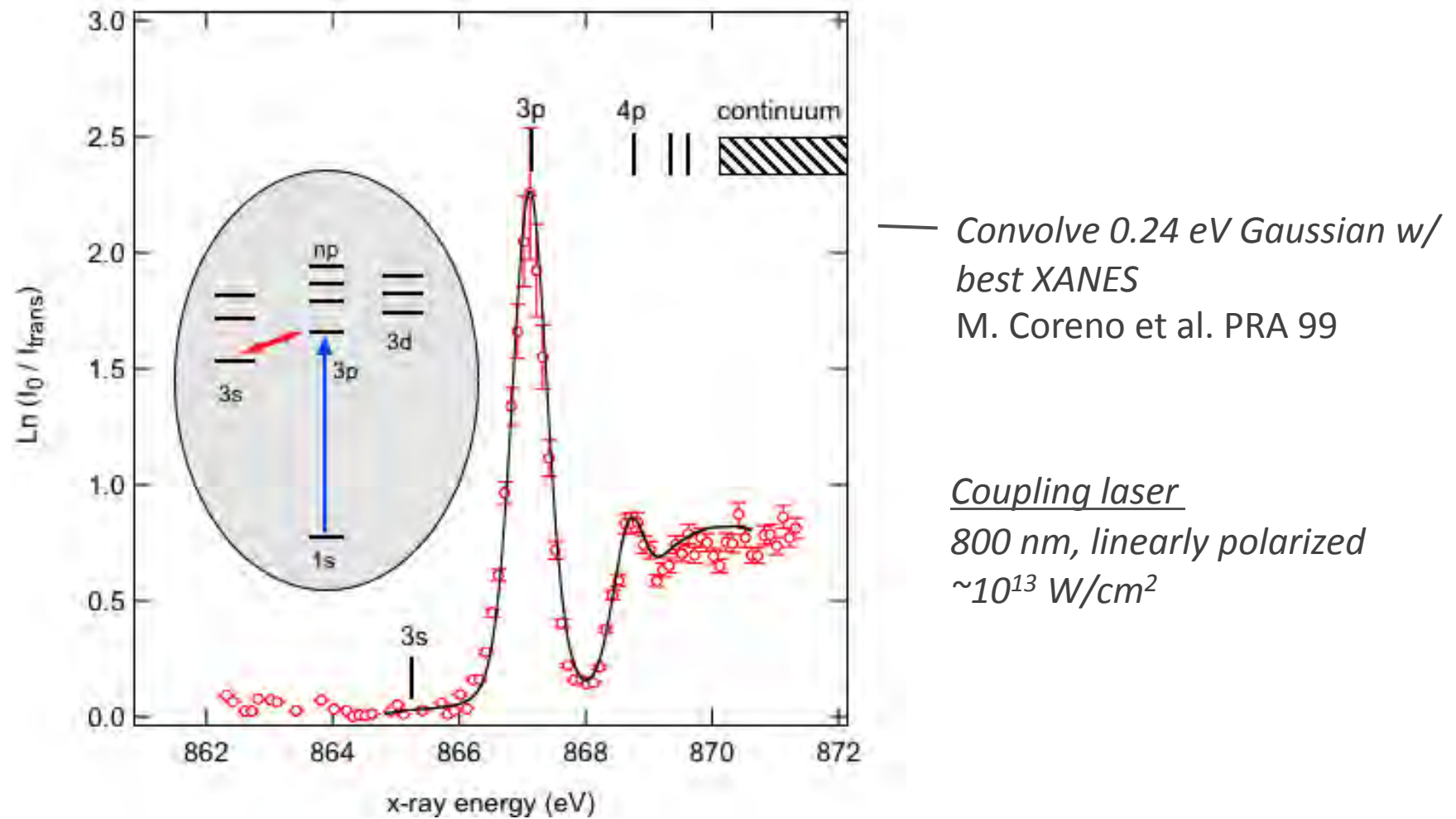
x-rays: $(54 \times 84.5 \mu\text{m}) (\text{H} \times \text{V})$, 225 fs

laser: $(80 - 150 \times 160 - 195 \mu\text{m}) (\text{H} \times \text{V})$, 290 fs

laser pulse energy (1.12, 0.80, or 0.50 mJ)



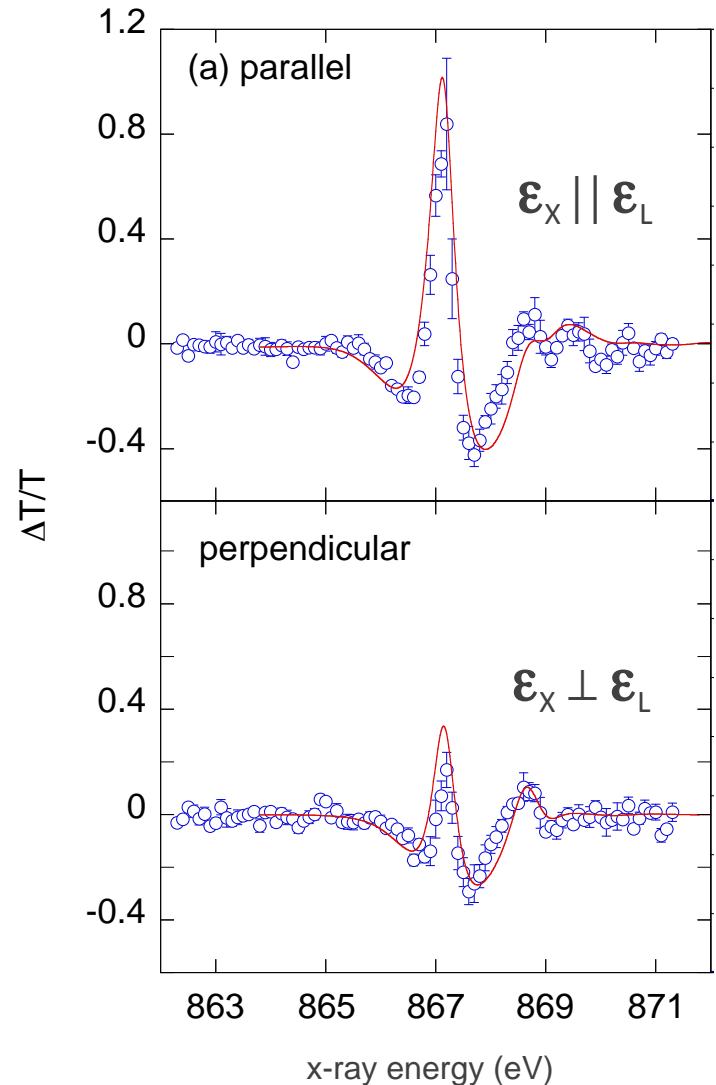
Neon absorption spectrum



Absorption spectrum w/ fs x-rays reproduces high resolution expt'l spectrum



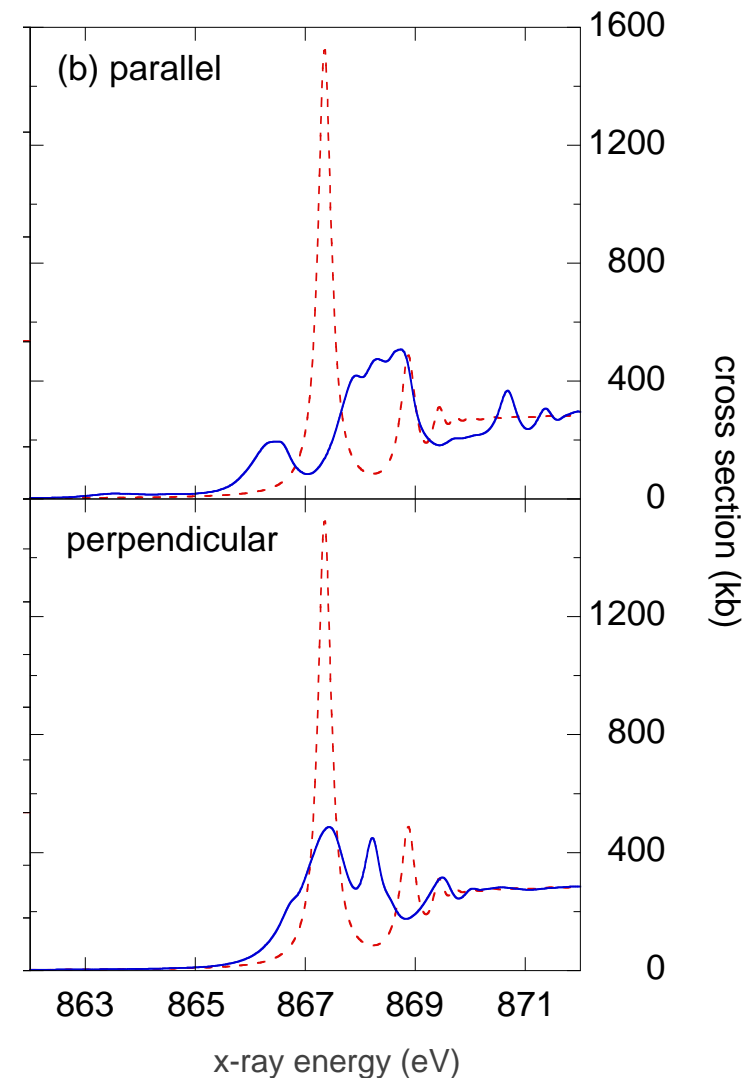
Observe EIT for x-rays



- *large effect (200-300%)*
- *induced transparency*
parallel >> perpendicular
- *1s-3p-3s subspace dominant*
- *excellent agreement with theory*
simulation with no adjustable parameters

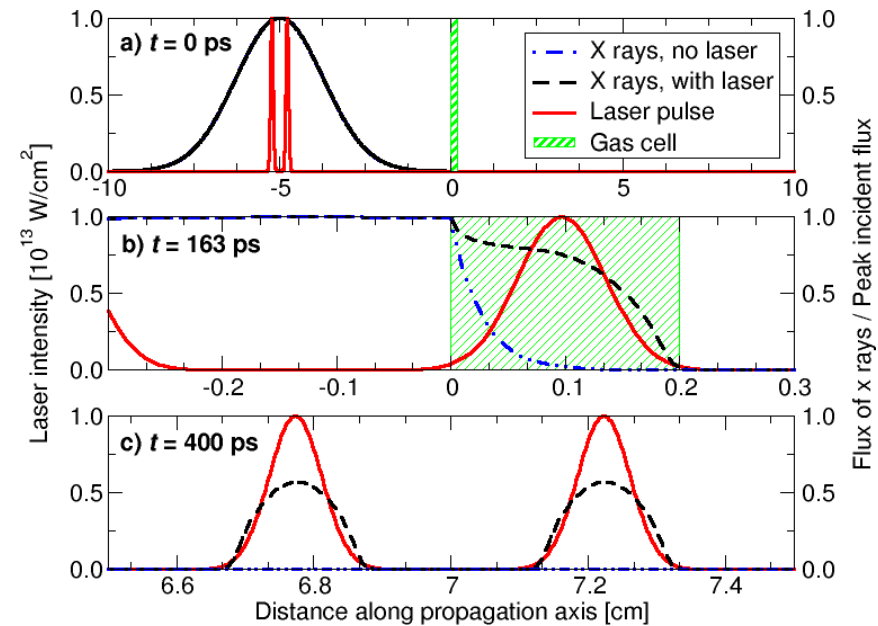
Simulation of x-ray propagation through laser-dressed media

- *Ab initio x-ray cross sections as fcn of laser intensity*
 $0.5 \times 10^{11} - 3 \times 10^{13} \text{ W/cm}^2$
- *Co-propagate x-rays and dressing laser through the medium*
 - x-ray spatial grid
41x41 transverse
51 longitudinal
 - 3900 time steps, 15.75 fs
 - 864-875 eV, 0.02 eV steps
- *X-ray transmission at each space time point*



Summary and outlook - EIT for x-rays

- Demonstrate control of photoelectric absorption of x-rays w/light
 - ultrafast, reversible x-ray switch
 - modifying the *final state*
 - predictive theoretical treatment
- Cross-correlation measurement of x-ray pulse width
- Imprint fs laser pulse shapes and sequences onto x-ray pulses



- Amplitude modulator for many wavelengths by multiplexing
- Extend to hard x-rays (Ar, Kr, Kr ions) - Butch & Santra PRA 08
- Control ratio of absorption to scattering





Strong field x-ray induced processes





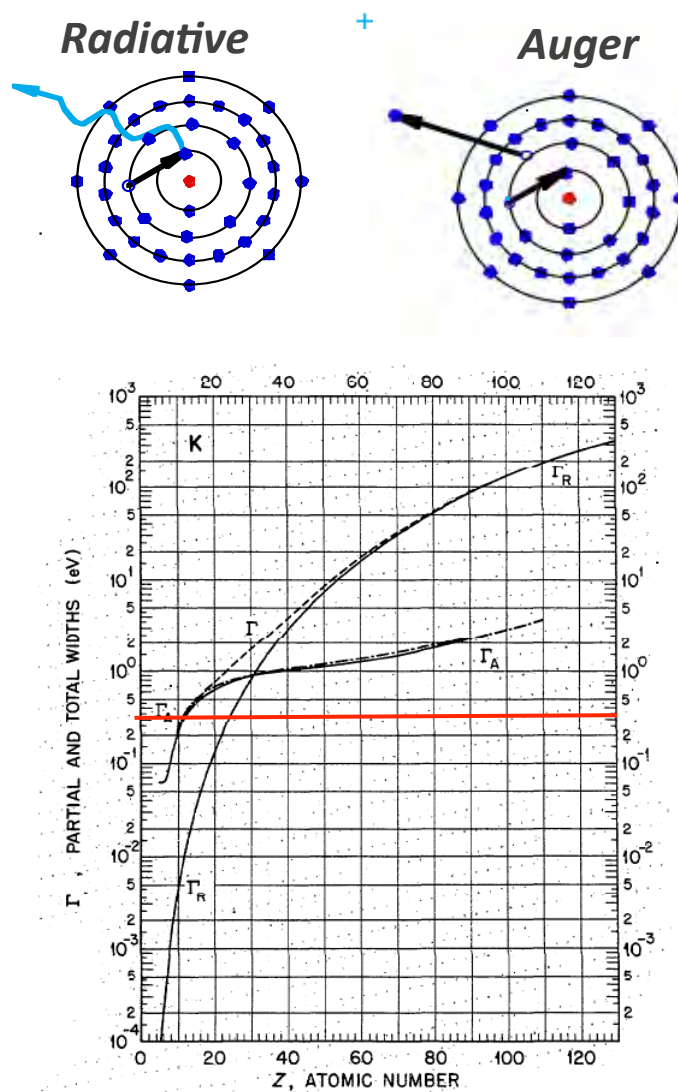
This exposition, for which we have previously established a conceptual foundation, provides a natural introduction to the nonlinear phenomena which are currently under investigation. The reader will discover that the latter have really been ready for discovery for many years, awaiting the techniques which could make them observable. They have counterparts in phenomena long known to specialists, but the intense beams and the precision and sensitivity of measurement which are essential to accurate description and prediction have come only recently.

G. C. Baldwin

An Introduction to Nonlinear Optics (1969).

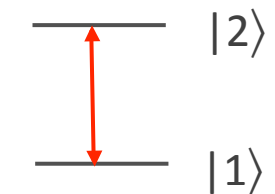


Intraatomic inner-shell decay vs x-ray-driven transitions



Rabi frequency

$$\Omega_{12} = \frac{\mu_{12} E}{\hbar}$$



$$\mu = er$$

$$1/\tau = \Omega_{12}$$

$$E_{\text{required}} = 1/\mu_{12}\tau$$

$$\mu_{\text{Ne } 1s-3p} = 0.01 \text{ } ea_0$$

$$\tau_{\text{Ne } 1s}^{-1} = 2.4 \text{ fs} = 100 \text{ a.u.}$$

$$E_{\text{Ne}} \sim 1 \text{ a.u.}$$

$$I_{\text{Ne}} \sim 3.4 \times 10^{16} \text{ W/cm}^2$$



Resonant Auger Decay of Molecules in Intense X-Ray Laser Fields: Light-Induced Strong Nonadiabatic EffectsLorenz S. Cederbaum,¹ Ying-Chih Chiang,¹ Philipp V. Demekhin,¹ and Nimrod Moiseyev²¹Theoretische Chemie, Universität Heidelberg, Im Neuenheimer Feld 229, 69120 Heidelberg, Germany²Schulich Faculty of Chemistry and Minerva Center, Technion—Israel Institute of Technology, Haifa 32000, Israel

(Received 21 September 2010; published 21 March 2011)

PHYSICAL REVIEW A 83, 023422 (2011)

Strong interference effects in the resonant Auger decay of atoms induced by intense x-ray fields

Philipp V. Demekhin* and Lorenz S. Cederbaum

Theoretische Chemie, Physikalisch-Chemisches Institut, Universität Heidelberg, Im Neuenheimer Feld 229, D-69120 Heidelberg, Germany

(Received 16 December 2010; published 25 February 2011)

PHYSICAL REVIEW A 81, 013812 (2010)

Propagation of a strong x-ray pulse: Pulse compression, stimulated Raman scattering, amplified spontaneous emission, lasing without inversion, and four-wave mixingYu-Ping Sun,^{1,2} Ji-Cai Liu,^{2,*} Chuan-Kui Wang,^{1,2} and Faris Gel'mukhanov²¹College of Physics and Electronics, Shandong Normal University, 250014 Jinan, People's Republic of China²Department of Theoretical Chemistry, School of Biotechnology, Royal Institute of Technology, S-10691 Stockholm, Sweden

(Received 29 July 2009; published 20 January 2010)

PHYSICAL REVIEW A 81, 043412 (2010)

Auger effect in the presence of strong x-ray pulsesJi-Cai Liu,^{1,2} Yu-Ping Sun,^{1,2,*} Chuan-Kui Wang,^{1,2} Hans Ågren,² and Faris Gel'mukhanov²¹College of Physics and Electronics, Shandong Normal University, 250014 Jinan, People's Republic of China²Theoretical Chemistry, School of Biotechnology, Royal Institute of Technology, S-106 91 Stockholm, Sweden

(Received 15 December 2009; published 19 April 2010)





Exploration of strong-field x-ray interactions has just begun!

